Development/Plasticity/Repair

# 5-$HT_4$ Receptor-Mediated Neuroprotection and Neurogenesis in the Enteric Nervous System of Adult Mice

**Min-Tsai Liu,[1] Yung-Hui Kuan,[4] Jingwen Wang,[2] René Hen,[3] and Michael D. Gershon[1]**

Departments of [1]Pathology and Cell Biology, [2]Biological Sciences, and [3]Neuroscience, Columbia University, New York, New York 10032, and [4]Max Planck Institute for Brain Research, 60528 Frankfurt, Germany

**Although the mature enteric nervous system (ENS) has been shown to retain stem cells, enteric neurogenesis has not previously been demonstrated in adults. The relative number of enteric neurons in wild-type (WT) mice and those lacking 5-$HT_4$ receptors [knock-out (KO)] was found to be similar at birth; however, the abundance of ENS neurons increased during the first 4 months after birth in WT but not KO littermates. Enteric neurons subsequently decreased in both WT and KO but at 12 months were significantly more numerous in WT. We tested the hypothesis that stimulation of the 5-$HT_4$ receptor promotes enteric neuron survival and/or neurogenesis. *In vitro*, 5-$HT_4$ agonists increased enteric neuronal development/survival, decreased apoptosis, and activated CREB (cAMP response element-binding protein). *In vivo*, in WT but not KO mice, 5-$HT_4$ agonists induced bromodeoxyuridine incorporation into cells that expressed markers of neurons (HuC/D, doublecortin), neural precursors (Sox10, nestin, Phox2b), or stem cells (Musashi-1). This is the first demonstration of adult enteric neurogenesis; our results suggest that 5-$HT_4$ receptors are required postnatally for ENS growth and maintenance.**

## Introduction

The enteric nervous system (ENS) resembles the CNS structurally and is able to control gut behavior in the absence of CNS input (Gershon and Tack, 2007). In contrast to the highly protected CNS, the ENS is exposed and subject to injury. Replacement of enteric neurons would thus seem to be important. The birth of enteric neurons has been demonstrated by pulse-chase administrations of tritiated thymidine ($^3$H-dT) or its analogues 5-bromo-2′-deoxyuridine (BrdU) to occur between embryonic day 8.5 (E8.5) and postnatal day 21 (P21) (Pham et al., 1991). Enteric neuronal stem cells, however, have been reported to be present in the postnatal murine bowel (Bixby et al., 2002; Kruger et al., 2002; Heanue and Pachnis, 2007). Although these cells would seem to be a potential source of new neurons, single pulses of BrdU have not been able to demonstrate birth of neurons in the adult ENS.

The bowel contains an extraordinarily high concentration of serotonin (5-HT) (Erspamer, 1966); moreover, the ENS expresses multiple 5-HT receptor subtypes, which regulate gastrointestinal (GI) motility and secretion (Galligan and Parkman, 2007). 5-HT has also been linked to the pathophysiology of irritable bowel syndrome and chronic constipation (CC), which can be treated with 5-$HT_4$ agonists (Gershon and Tack, 2007). These compounds presynaptically enhance secretion of acetylcholine and calcitonin gene-related peptide, increase the amplitude of EPSCs, and strengthen neurotransmission in prokinetic pathways. CC, however, is associated with an age-related decline in neuronal numbers (Camilleri et al., 2008); therefore, if 5-$HT_4$ agonists were to counteract this decline, that might contribute to their efficacy in the treatment of CC. 5-$HT_4$ receptors appear early in fetal life and are abundant in the ENS (Gershon and Ratcliffe, 2006). 5-$HT_4$ receptors are coupled to Gs, and increase cAMP (Dumuis et al., 1989a,b; Bockaert et al., 2004, 2008). Stimulation of 5-$HT_4$ receptors has been shown to stimulate neurogenesis in the hippocampus and to produce antidepressant-like effects (Lucas et al., 2007).

We tested the hypotheses that 5-$HT_4$ receptors enhance survival and/or neurogenesis in the adult ENS *in vivo*. We show that, in wild-type (WT) mice, relative numbers of enteric neurons increase through 4 months of age but decline thereafter. In mice lacking 5-$HT_4$ receptors [knock-out (KO)], however, the early increase fails to occur and the later decline is more severe. 5-$HT_4$ receptors specifically protect cultured enteric neurons from apoptosis and also activate cAMP response element-binding protein (CREB). 5-$HT_4$ agonists promote the generation of enteric neurons in adult WT mice but not in their KO littermates. This is the first demonstration of the mobilization of progenitor cells *in vivo* to give rise to neurons in the adult ENS.

## Materials and Methods

*Animals.* The 5-$HT_4$ KO and WT mice (SvEv129) were bred at Columbia University and some WT mice were purchased from Charles River Laboratories. The generation and characterization of 5-$HT_4$ KO mice has previously been reported (Compan et al., 2004). Genotypes were determined by PCR analysis of mouse tail DNA. Exposure to $CO_2$ was used for killing. Procedures and care followed guidelines of the National Institutes of Health and were approved by the Animal Care and Use Committee of Columbia University.

Received March 9, 2009; revised May 18, 2009; accepted June 19, 2009.

This work was supported by National Institutes of Health Grants NS12969 and NS15547 and Novartis. We thank Wanda Setlik for electron microscopy, and Dr. Valerie Compan, who originally derived mice that lack 5-$HT_4$ receptors in the laboratory of René Hen.

Correspondence should be addressed to Min-Tsai Liu, Department of Pathology and Cell Biology, College of Physicians and Surgeons, Columbia University, 630 West 168th Street, Box 23, New York, NY 10032. E-mail: ml27@columbia.edu.

DOI:10.1523/JNEUROSCI.1145-09.2009

 0270-6474/09/299683-17$15.00/0

*Gastrointestinal motility.* Animals were starved overnight (>16 h) and deprived of water for 2 h before each experiment. Dextran (6.5 mg/ml) conjugated to fluorescein or rhodamine B (70,000 $M_r$; Invitrogen) was dissolved in saline and administered by gavage in a volume of 0.1 ml. The bowel (stomach to colon) was removed 20 or 45 min after gavage. The stomach was examined as a unit; the small intestine was divided into 10 equal segments. The cecum was separated from the rest of the colon, which in turn was divided into proximal and distal halves. Each segment of gut was placed in 4 ml of filtered 0.9% NaCl and shaken vigorously for ~1 min to remove luminal contents. The resulting suspension was clarified by centrifugation (2700 rpm; 20 min; 4°C), and its fluorescence intensity was measured in duplicate aliquots. The total amount of fluorescent dextran recovered from each mouse was determined. The proportion of the total remaining in the stomach when the mouse was killed was then used to calculate gastric emptying (GE), which was defined as follows: % GE = [(total fluorescence recovered − residual fluorescence in the stomach) ÷ (total fluorescence recovered)] × 100%. To estimate small intestinal motility, the geometric center (GC) of fluorescence intensity in the small intestine was measured. For this purpose, the total of the measured intensities of fluorescence ($\phi$) in each segment of small intestine was calculated. The geometric center was defined as follows: GC = [$\Sigma$ ($\phi$ × segment number)] ÷ total fluorescence recovered in small intestine. Gastric emptying and the GC of small intestinal fluorescence were calculated for 5-HT$_4$ KO mice and their WT littermates, which served as matched controls. In no experiment did significant quantities of fluorescent dextran reach the colon.

*Immunocytochemical procedures.* Small and large intestine were removed and fixed with 4% formaldehyde (from paraformaldehyde) in 0.1 M phosphate buffer, pH 7.4. Laminar preparations were dissected and analyzed as whole mounts of longitudinal muscle with adherent myenteric plexus (LMMP). Endogenous peroxidase activity was blocked by incubating preparations with 3% $H_2O_2$ for 20 min at room temperature. Endogenous biotin was blocked with a commercial streptavidin/biotin blocking kit (Vector Laboratories) according to manufacturer's instruction. For chicken antibodies, nonspecific staining was blocked with BlokHen II (diluted 1:10 in PBS; 20 min; room temperature; Aves Labs). Incubation with blocking solution (45 min at room temperature), primary or secondary antibodies was performed in PBS with 10% normal horse serum (NHS) (Invitrogen) and 1% Triton X-100 (0.3% for cultured cells). Primary antibodies were applied overnight (>16 h) at room temperature (Table 1). After washing with PBS, sites of bound primary antibodies were detected by incubation with secondary antibodies (Table 2) for 3 h at room temperature. Control sections were incubated only with secondary antibodies. Bisbenzimide (Sigma-Aldrich; 1 $\mu$g/ml in distilled $H_2O$ for 1 min at room temperature) was used to stain DNA. After immunostaining, preparations were washed with PBS and mounted in fade-resistant media (Vectashield; Vector Laboratories).

Slides were examined with a Leica DMR RXA2 microscope equipped with a cooled CCD camera (Retiga EXi; QImaging) and computer-assisted video imaging system programs (OpenLab 5 and Volocity 5; Improvision). Measured parameters were quantified with computer assistance using the ImageJ program (W. S. Rasband, ImageJ, National Institutes of Health, Bethesda, MD; http://rsb.info.nih.gov/ij/; 1997–2007). Contrast of digital images was adjusted using Adobe Photoshop software (Adobe Systems), which were also used to arrange images in figures. No other image manipulations were used.

*Isolation of enteric crest-derived cells and adult myenteric neurons.* All enteric neurons and glia are derived ontogenetically from the neural crest (Le Douarin and Kalcheim, 1999). Crest-derived cells migrate to and colonize the fetal gut. Crest-derived cells were p75$^{NTR}$-immunoselected from fetal bowel (Pomeranz et al., 1993), and the isolated crest-derived cells then give rise to enteric neurons and glia *in vitro*. Fetal mouse intestines (E12) were obtained from WT mice, removed by dissection in 0.357% HEPES-buffered HBSS, pH 6.2 (Invitrogen), and pooled. The intestines were then dissociated with collagenase A (1 mg/ml; Roche Diagnostics; catalog #11088785103) in HBSS for 30 min at 37°C water bath, triturated, and centrifuged at 1000 rpm for 3 min to collect cells. The pellet was suspended with 10% heat-inactivated horse serum in Neurobasal medium (Invitrogen) and incubated with rabbit polyclonal antibodies to p75$^{NTR}$ on ice for 1 h with gentle agitation. After centrifuging and washing with Neurobasal medium, the pellet was resuspended and incubated with goat antibodies to rabbit IgG, which were coupled to magnetic microbeads (50 $\mu$l per $10^7$ cells; Miltenyi Biotec). Incubation

**Table 1. Primary antibodies used for immunocytochemistry**

| Antigen | Host species | Dilution | Sources |
|---|---|---|---|
| $\beta$3-tubulin | Rabbit | 1:1000 | Covance; PRB-435P |
| B-FABP | Rabbit | 1:1000 | Gift from T. Müller (Max Delbrück Center for Molecular Medicine, Berlin, Germany) |
| BrdU (BU-1) | Mouse IgG$_{2a}$ | 1:100 | GE Healthcare; RPN202 |
| BrdU [BU1/75 (ICR1)] | Rat IgG$_{2a}$ | 1:50 | AbD Serotec; MCA2060 |
| CREB (48H2) | Rabbit | 1:400 | Cell Signaling; 9197 |
| Phospho-CREB (87G3) | Rabbit | 1:25 | Cell Signaling; 9198 |
| Doublecortin (C-18) | Goat | 1:50 | Santa Cruz; sc-8066 |
| GFAP | Chicken IgY | 1:2000 | Neuromics; CH22102 |
| HuC/D | Mouse-biotin | 1:50 | Invitrogen; A21272 |
| HuD (N-15) | Goat | 1:100 | Santa Cruz; sc-5977 |
| Ki67 (SP6) | Rabbit | 1:80 | Vector Laboratories; VP-RM04 |
| LC3B | Rabbit | 1:800 | Novus; NB600-1384 |
| LC3B | Rabbit | 1:1000 (WB) | Sigma-Aldrich; L7543 |
| Musashi-1 | Rabbit | 1:100, 1:1000 (WB) | Neuromics; RA14128 |
| Nestin | Rabbit | 1:100 | Gift from R. D. Goldman (Department of Cell and Molecular Biology, Northwestern University, Chicago, IL) |
| Neurofilament-H | Chicken IgY | 1:2000 | Neuromics; CH22104 |
| nNOS | Rabbit | 1:1000 | Santa Cruz; sc-648 |
| p75$^{NTR}$ | Rabbit | 1:500 | Gift from M. V. Chao (Skirball Institute of Biomolecular Medicine, New York University, New York, NY) |
| Peripherin (C-19) | Goat | 1:1000 | Santa Cruz; sc-7604 |
| PGP9.5 | Rabbit | 1:1000 | AbD Serotec; 7863-0504 |
| Phox2b | Rabbit | 1:500 | Gift from J. F. Brunet (École Normale Supérieure, Département de Biologie, Paris, France) |
| S100$\beta$ | Rabbit | 1:1000 | Neuromics; RA25022 |
| Sox10 | Guinea pig | 1:500 | Gift from M. Wegner (Institut für Biochemie, Universität Erlangen-Nürnberg, Erlangen, Germany) |
| Synaptotagmin | Rabbit | 1:1000 | Sigma-Aldrich; S2177 |
| $\alpha$-Tubulin (DM1A) | Mouse IgG$_1$ | 1:4000 (WB) | Millipore; 05-829 |

WB, Western blotting.

**Table 2. Secondary antibodies used for immunocytochemistry**

| Antibody | Dilution | Sources |
|---|---|---|
| Donkey anti-chicken IgY fluorescein | 1:100 | Jackson ImmunoResearch; 703-095-155 |
| Donkey anti-goat IgG Alexa Fluor 488 | 1:400 | Invitrogen; A11055 |
| Donkey anti-goat IgG Alexa Fluor 594 | 1:400 | Invitrogen; A11058 |
| Donkey anti-rabbit IgG Alexa Fluor 350 | 1:400 | Invitrogen; A10039 |
| Donkey anti-rabbit IgG Alexa Fluor 488 | 1:400 | Invitrogen; A21206 |
| Donkey anti-rabbit IgG Alexa Fluor 594 | 1:400 | Invitrogen; A21207 |
| Donkey anti-rat IgG Alexa Fluor 594 | 1:400 | Invitrogen; A21209 |
| Donkey anti-mouse IgG IRDye 800 | 1:8000 (WB) | Rockland Immunochemicals; 610-732-124 |
| Goat anti-guinea pig IgG Alexa Fluor 488 | 1:400 | Invitrogen; A11073 |
| Goat anti-mouse IgG$_{2a}$ Cy3 | 1:400 | Jackson ImmunoResearch; 115-165-206 |
| Goat anti-rabbit IgG Alexa Fluor 680 | 1:400<br>1:8000 (WB) | Invitrogen; A21109 |
| Streptavidin Alexa Fluor 350 | 1:100 | Invitrogen; S11249 |
| Streptavidin Alexa Fluor 488 | 1:100 | Invitrogen; S11223 |
| Streptavidin Alexa Fluor 680 | 1:100 | Invitrogen; S32358 |

WB, Western blotting.

was performed in a degassed Neurobasal medium with 0.5% BSA (Sigma-Aldrich) for 15 min at 4°C. The antibody-decorated cells were then passed through columns (Miltenyi Biotec) in a magnetic field according to the manufacturer's directions. Crest-derived cells are retained on the column and non-crest-derived cells pass through. The magnetic field was then removed; the crest-derived cells were flushed from the column in degassed Neurobasal medium and grown in culture. Cells were plated at densities of $1.0 \times 10^5$ cells/ml in Neurobasal medium supplemented, for plating overnight, with 10% heat-inactivated horse serum. The cells were finally cultured in serum-free feeding medium.

Methods for culturing neurons from the ENS of adult mice have been described previously (Liu et al., 2002). Briefly, the LMMP was dissected from the intestines of adult male mice (at the age of 6–8 weeks). The preparations were pooled and dissociated with collagenase (1.5 mg/ml; Worthington Biochemicals; catalog #LS004204) in Krebs' solution (in mM: 121.3 NaCl, 5.95 KCl, 14.3 $NaHCO_3$, 1.34 $NaH_2PO_4$, 1.2 $MgCl_2$, 2.5 $CaCl_2$, and 12.7 glucose, pH 7.4) at 37°C for 60 min. The digested tissue was triturated and centrifuged at 2100 rpm for 5 min at room temperature to collect cells. The pelleted cells were resuspended in plating medium [10% heat-inactivated fetal bovine serum in DMEM/F12 (Invitrogen)] and plated at densities of $1.5 \times 10^5$ cells/ml. After 6 h, the medium was changed to serum-free feeding medium.

*Neuronal culture.* Enteric neurons were isolated from fetal and adult bowel and cultured at medium density. Suspended cells were plated on 12 mm round coverslips (Warner Instruments), 16-well glass chamber slides (Nalge Nunc), or flat-bottomed 96-well dishes (Corning Life Sciences) coated with poly-L-lysine HBr (20 μg/ml; Sigma-Aldrich) and Matrigel (1:10 dilution; BD Biosciences). The serum-free feeding medium consisted of Neurobasal for prenatal or Neurobasal A for adult neural cultures, supplemented with B27 (1:50 dilution; Invitrogen), L-glutamine (0.1 mg/ml; Invitrogen), epidermal growth factor (EGF) (20 ng/ml; Alomone Labs), basic fibroblast growth factor (bFGF) (20 ng/ml; Alomone Labs), and 1% penicillin/streptomycin/antimycotic (Invitrogen) and gentamicin (50 μg/ml; Invitrogen). Cells were incubated at 37°C in 5% $CO_2$ and fed every 2 d until used for experiments. After experimental procedures, cultures were fixed for 20 min and processed for immunostaining and/or in-cell ELISA (used triplicate samples).

Cultures of $p75^{NTR}$-immunoselected cells were allowed to rest under basal conditions for 2 d. The media were then supplemented with 5-$HT_4$ receptor agonists [1-(4-amino-5-chloro-2-methoxyphenyl)-3-[1–2-methylsulphonylamino)ethyl-4-piperidinyl]-1-propanone hydrochloride (RS67506) or tegaserod] in concentrations of 0.1, 1.0, 10, and 100 nM, and the cells were cultured for an additional 48 h. EGF and bFGF were omitted from the medium. Other cultures were treated with a 5-$HT_4$ antagonist [1-methyl-1*H*-indole-3-carboxylic acid, [1-[2-[(methylsulfonyl)amino]ethyl]-4-piperidinyl]methyl ester (GR113808); 10 nM], which was added by it or together with 5-$HT_4$ agonists. After 2 d of incubation with 5-$HT_4$ agonists and/or GR113808, cells were rinsed in PBS and fixed immediately with 4% formaldehyde (from paraformaldehyde) for immunocytochemical analyses with antibodies to β3-tubulin.

Cultures from adult bowel were allowed to rest under basal conditions at 37°C for 2 d. They were then transferred to Opti-MEM I medium (Invitrogen) and starved for 12–16 h. On the day of experiment, the medium was supplemented with 5-$HT_4$ receptor agonists (RS67506 or tegaserod) in concentrations 0.1, 1.0, 10, and 100 nM. When responses to potential inhibitors were to be studied, the experimental compound was added by itself or together with the 5-$HT_4$ agonists. When combined, the antagonist was applied 30 min before the addition of 5-$HT_4$ agonists and the incubation was terminated after an additional 20 min. The potential inhibitors investigated included the 5-$HT_4$ antagonists, GR113808 or (1-butyl-4-piperidinyl)methyl-8-amino-7-chloro-1,4-benzodioxane-5-carboxylate hydrochloride (SB204070) (10 nM). Cells were rinsed with PBS and fixed for 20 min with 4% formaldehyde [supplemented with a phosphatase inhibitor mixture (Roche)]. Cultures were analyzed for phosphorylated CREB (pCREB) either by immunocytochemistry or by means of in-cell ELISA (FACE Maker; Active Motif), used according to the manufacturer's recommendations.

*Cell death assay.* The terminal deoxynucleotidyl transferase-mediated dUTP nick-end labeling (TUNEL) assay was used to detect apoptosis *in vitro*. The *in situ* cell death fluorescein detection kit from Roche was used for TUNEL assays according to the manufacturer's directions. Neurons were marked first by immunostaining β3-tubulin and the TUNEL assay was performed afterward. When the TUNEL analysis was to be applied to whole mounts, the preparations were first permeabilized with proteinase K (20 μg/ml in PBS; Roche) for 15 min at 37°C. Counts were normalized to the total number of cells, which was determined by counting bisbenzimide-stained nuclei.

*Electron microscopy.* Colons were removed from mice (at the age of 6–8 weeks), which had been perfused with a mixture of 4% formaldehyde (from paraformaldehyde), 2.5% glutaldehyde, and 1.25 mM $CaCl_2$ in 0.1 M cacodylate buffer, pH 7.2. Segments of colon were postfixed with 4% osmium tetroxide, washed, and stained en bloc with 2% uranyl acetate in 70% ethanol. The blocs were then dehydrated, cleared with propylene oxide, and flat embedded in Epon 812 (Electron Microscopy Sciences), which was polymerized at 60°C. Ultrathin sections were collected on Formvar-coated nickel grids, stained with uranyl acetate and lead citrate, and examined with a JEOL 1200EX electron microscope.

*Detection of newborn neurons* in vivo. A micro-osmotic pump (Alzet; catalog #AP-1007D; Durect Corporation), surgically implanted into the abdominal cavity of mice, was used to deliver BrdU diluted from a stock solution of BrdU, which dissolved in alkaline saline (15 mg/ml BrdU in 0.007N NaOH/0.9% NaCl; Millipore). BrdU was infused at a rate of ~30 $mg \cdot kg^{-1} \cdot d^{-1}$ for 7 d and was applied in the absence (vehicle control) or presence of tegaserod or RS67506 (11.4 fmol/d), which were dissolved in dimethyl sulfoxide (DMSO) and diluted in saline. Tegaserod or RS67506 were also given in the animals' drinking water (100 nM) during the post-BrdU chase (for as long as 10 weeks). To identify cells that incorporated BrdU, type-specific antibodies were applied before anti-BrdU (Table 1). The primary marker used to demonstrate cells differentiating in a neuronal lineage was antibodies to HuC/D. Antibodies to the neuronal nuclear protein (NeuN), which are often used for this purpose in the CNS, in which these antibodies label the nuclei of mature neurons (Mullen et al., 1992; Wang et al., 2008), cannot be used as a general neuronal marker in the ENS; NeuN is not expressed by all enteric neurons (Chiocchetti et al., 2003; Van Nassauw et al., 2005). DNA was denatured in whole mounts of tissue with 0.1N HCl (37°C for 5 min), followed by neutralization with 0.1 M sodium borate buffer, pH 8.5 (5 min), washing with PBS (three times), incubation with DNase-1 (GE Healthcare) with antibodies to BrdU for 1 h at room temperature. Subsequent steps included washing three times with PBS, blocking (30 min), and incubation with appropriate secondary antibodies. PBS, with added 10% NHS, 5% fetal calf serum (FCS) (HyClone), and 1% Triton X-100, was used for blocking and incubation with antibodies. BrdU was also quantified in cells freshly isolated from LMMP preparations dissected from the same animals that were used for immunocytochemical analyses. LMMPs were pooled, dissociated with collagenase, and cultured overnight, and in-cell ELISA (Biotrak Cell Proliferation ELISA kit; GE Healthcare) was used to measure the total amount of incorporated BrdU. Triplicate samples were assayed.

*Protein extraction and immunoblots.* Tissues were isolated and frozen immediately in liquid $N_2$ and stored at −80°C. Frozen samples were thawed and homogenized in ice-cold lysis buffer, containing 20 mM Tris-HCl, pH 7.5, 150 mM NaCl, 0.1% Triton X-100, 1 mM dithiothreitol (Sigma-Aldrich), 1 mM phenylmethylsulfonyl fluoride (Sigma-Aldrich), and protease inhibitor mixture with 1 mM EDTA (Roche). The resulting homogenates were then passed several times through a 22 gauge needle and incubated for 15 min on ice. The lysate was centrifuged at 13,000 rpm for 15 min at 4°C and the protein content of the supernatant was quantified (Bradford protein assay; Bio-Rad). Membrane proteins were extracted by using ProteoExtract kit (EMD Chemicals). Aliquots containing 20 μg of total protein were diluted with 6× Laemmli sample buffer, boiled for 5 min, loaded onto a 4–20% polyacrylamide gel (Pierce), and subjected to electrophoresis along with the prestained Precision Plus Blue Standard (Bio-Rad). The separated proteins were immobilized by electrotransfer to nitrocellulose membranes (0.2 μm pore; Li-Cor; Li-Cor Biosciences). After blocking nonspecific binding sites

with 5% nonfat dry milk solids (Bio-Rad) in Tris-buffered saline (TBS), pH 7.4, for 1 h, membranes were incubated with 5% FCS in TBS with 0.1% Tween 20 (TBST) for 30 min at room temperature, and probed overnight at 4°C with primary antibodies (Table 1). After three washes in TBST, secondary antibodies (0.2 $\mu$g/ml) (Table 2) were applied at room temperature for 1 h, followed by three washes in TBST and two washes in PBS. All incubation steps with primary or secondary antibodies were performed in TBST with 5% FCS. An infrared imaging system (Odyssey; Li-Cor) was used to examine the immunoblots. Relative signal intensity was quantified with NIH ImageJ software.

*Optical measurements and analysis.* Measured parameters were quantified with computer assistance using the ImageJ program to count neurons and measure Feret's diameters. Feret's diameter is defined as a microscopic term applying to the measured distance between theoretical parallel lines that are drawn tangent to the particle profile and perpendicular to the ocular scale. A simple way to explain Feret's diameter is that it is the longest distance between any two points along the region of interest boundary, also known as maximum caliper (ImageJ program; http://rsb.info.nih.gov/ij/). Object threshold analysis was used to outline each neuron in the analyzed myenteric ganglion. Neurons that overlapped were split manually to assure that accurate counts were obtained; however, overlapping neurons were omitted when Feret's diameters were measured. Neurite length was estimated with an ImageJ plug-in for the NeuronJ software program (Abràmoff et al., 2004). Three-dimensional reconstructions of myenteric ganglia in whole-mount preparations were obtained by deconvolution of images photographed in a *Z*-stack of focal planes (0.25 $\mu$m). Volocity 4 (Improvision) was used for deconvolution and three-dimensional reconstruction of images.

In tissue culture preparations, neurons were assessed morphometrically in uniform areas, which were selected at random in cell-containing regions. Parameters included counts of the number of neurons per square millimeter and measurements of the length of neurites. Neurite length was defined as the distance from the boundary of the cell body to the tip of the longest branch of each identifiable neurite. Cells were omitted from the analyses when neurites of adjacent neurons overlapped so as to confound measurements by making it difficult to assign neurites to a given neuron. Comparisons were always made between cultures established at the same time. In whole mounts of LMMP, ganglia were identified and photographed using a 10× objective. Fields were randomly selected for analysis; however, care was taken to be certain that the entire circumference of the bowel was sampled. Numbers of neurons were normalized to the total area examined (in square millimeters). Laminar preparations obtained from KO mice were compared with their WT littermates. Numbers obtained in this way are relative because no attempt was made to estimate the total numbers of myenteric neurons present in the colon. Preparations to be compared were immunostained simultaneously and analyzed using the same fluorescence threshold adjustments. For each tissue culture well and for each whole-mount segment, 10 microscopic fields were analyzed. For every experiment, at least three cultures or LMMP preparation of each type were analyzed and statistical comparisons were made between three and six independent experimental groups.

*Statistical analysis.* Data were expressed as means ± SEM. Means were statistically compared by one-way ANOVA with Bonferroni's *post hoc* multiple-comparison tests of differences (Prism; GraphPad Software). Alternatively, an unpaired two-tailed Student *t* test was used when only two means were compared. In either case, $p < 0.05$ was taken as the level of statistical significance.

*Compounds used.* Drugs were prepared as stock solutions in distilled water, ethanol, or DMSO (Sigma-Aldrich) at $>10^3$ times the highest experimental concentration to be used. Stock solutions were stored at −20°C until used. In experiments, stock solutions of compounds were diluted in culture medium or for, *in vivo* use, saline. RS67506, GR113808, and *N*-[2-[[3-(4-bromophenyl)-2-propenyl]amino]ethyl]-5-isoquinolinesulfonamide dihydrochloride (H89) were obtained from Tocris. SB204070 was purchased from Sigma-Aldrich. Tegaserod was obtained from Novartis.

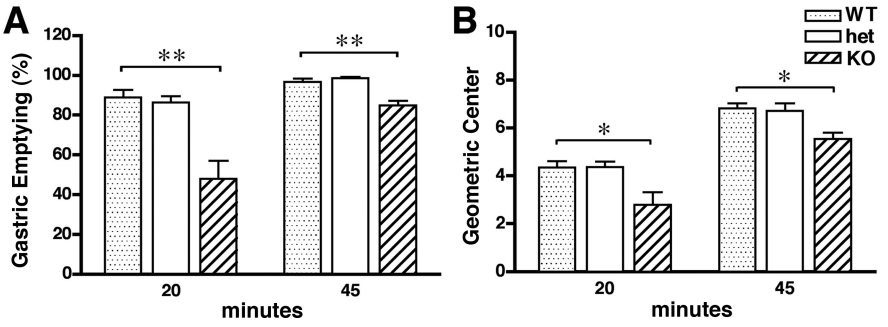


**Figure 1.** Deletion of 5-HT$_4$ receptors delays gastric emptying and small intestine transit. ***A***, The rate of GE, measured with fluorescent dextran, did not differ in WT and 5-HT$_4$+/− (het) mice but was significantly delayed in KO animals (**$p < 0.01$). ***B***, The transit of fluorescent dextran, measured as the GC, was similar in WT and het mice but was significantly retarded in KO animals (*$p < 0.05$). The number of mice (at the age of 8 weeks) per group at 20 min was 5 (WT), 8 (het), 4 (KO), and, at 45 min, 7 (WT), 10 (het), and 6 (KO). Error bars indicate SEM.

## Results

### Gastric emptying is delayed and small intestine transit time is slow in KO mice

Fluorescent dextran was administered to 2-month-old WT, 5-HT$_4$+/− (het), and KO mice by gavage to estimate the efficiency of gastric emptying and small intestinal transit (Miller et al., 1981; Moore et al., 2003; Inada et al., 2004). To evaluate GE, the probe remaining in the stomach was determined after 20 or 45 min, whereas small bowel transit time was measured by determining the GC of the fluorescent dextran that had moved into the small intestine. GE was significantly less efficient in KO than in WT and het mice ( $p < 0.01$) (Fig. 1*A*); however, GE was similar in WT and het mice. Intestinal transit was also significantly slower in KO than in WT or het mice ( $p < 0.05$) (Fig. 1*B*), and again, intestinal transit was similar in WT and het animals. It is interesting that gastric emptying and small bowel transit in 5-HT$_4$+/− mice are equivalent to those of WT animals; therefore, it is likely that one-half of the protein is sufficient to maintain function. These observations indicate that 5-HT$_4$ receptors play a physiological role in gastric emptying and small bowel transit in adult mice.

### The number and the size of myenteric neurons decrease as a function of age in KO mice

The densities of myenteric neurons in the colons of WT mice was determined and compared with those of KO mice at 1, 4, and 12 months of age. Antibodies to HuC/D were used to demonstrate neurons in whole mounts of LMMP (Fig. 2*A–F*). HuC/D is an RNA-binding protein that begins to be expressed soon after neural differentiation and continues to be expressed through adulthood (Marusich and Weston, 1992; Barami et al., 1995). In the developing ENS, HuC/D immunoreactivity is acquired early in development when proliferating crest-derived precursors differentiate into enteric neurons (Young et al., 2005; D'Autréaux et al., 2007) and, in the adult bowel, is a specific neuronal marker (Graus et al., 1985; Okano and Darnell, 1997; Phillips et al., 2004; Ganns et al., 2006). Colonic HuC/D-immunoreactive neurons were counted by using ImageJ program. At 1 month of age, the densities of colonic myenteric neurons in WT and KO mice were

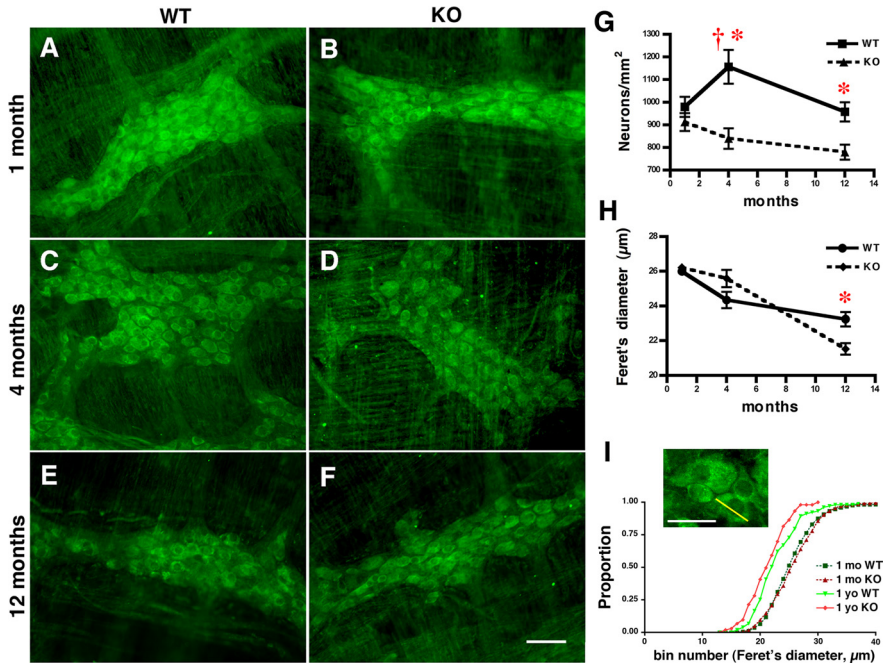


**Figure 2.** The number and the size of myenteric neurons decrease as a function of age in colons of KO mice. ***A–F***, Antibodies to HuC/D demonstrate myenteric neurons in LMMP from colons of WT (***A***, ***C***, ***E***) and KO (***B***, ***D***, ***F***) mice at 1 (***A***, ***B***), 4 (***C***, ***D***), and 12 months (***E***, ***F***). Scale bar, 50 $\mu$m. ***G***, In WT mice, numbers of myenteric neurons increase between 1 and 4 months ($^{\dagger}p < 0.05$); numbers then decrease between 4 and 12 months ($p < 0.05$). In KO mice, numbers of myenteric neurons decline linearly between months 1 and 12 ($p < 0.05$). Although neuronal numbers are similar in WT and KO mice at 1 month ($n = 40$), KO mice have fewer neurons at 4 months ($n = 20$) and 12 months of age ($n = 41$) ($^{*}p < 0.01$). ***H***, Feret's diameter of WT and KO mice did not differ significantly at 1 ($n = 830$) or 4 months ($n = 103$). But Feret's diameter of colonic myenteric neurons declines significantly between 1 and 12 months in both WT and KO mice ($p < 0.01$); however, at 12 months, Feret's diameter was significantly smaller in KO mice ($n = 103$) ($^{*}p < 0.01$). The number of mice per group was three at least. Error bars indicate SEM. ***I***, Frequency distribution of the proportion of Feret's diameters of myenteric neurons in WT and KO mice at 1 and 12 months of age. There is an age-associated shift to the left that is greater in KO than WT mice. Inset, High-magnification image of neurons immunostained with antibodies to HuC/D from which Feret's diameters (yellow line drawn on a typical neuron) were measured with ImageJ software. Scale bar, 50 $\mu$m.

not significantly different (Fig. 2*G*). Between 1 and 4 months, however, the relative number of myenteric neurons increased in WT ($p < 0.05$) but not in KO mice (Fig. 2*G*); therefore, at 4 months, more neurons were present in WT than in KO animals ($p < 0.01$) (Fig. 2*G*). Between 4 and 12 months, myenteric neurons were lost in the WT colon ($p < 0.01$); nevertheless, because the relative number of neurons also declined between 1 and 12 months in KO animals (Fig. 2*G*), the 12-month-old WT colon contained significantly more myenteric neurons than that of KO mice ($p < 0.01$) (Fig. 2*G*). The number of neurons in the mammalian ENS is known to decline late in life (Santer and Baker, 1988; Johnson et al., 1998; Gabella, 2001; Wade and Cowen, 2004; Phillips and Powley, 2007). Most studies of this phenomenon have compared young adult to extremely old animals. The current observations suggest that an early postnatal increase in myenteric neurons precedes the later decline in numbers that begins during the first year of life. A major difference between WT and KO mice is that the earlier increment in neurons is deficient in KO animals, which thus are less well prepared for the age-related decline that ultimately occurs in both WT and KO mice. These data are consistent with the idea that 5-HT$_4$ receptors play a role in the postnatal generation of enteric neurons.

Feret's diameter (the longest diameter that can be measured in a neuron) was determined in HuC/D-expressing myenteric neurons. Feret's diameters of colonic myenteric neurons did not differ significantly in WT and KO mice at 1 or 4 months of age (Fig. 2*H*). At 12 months, however, Feret's diameter was significantly smaller in KO mice than in their WT littermates ($p < 0.01$) (Fig. 2*H*). Feret's diameter declined significantly between 1 and 12 months of age in both WT and KO mice ($p < 0.01$) (Fig. 2*H*); however, the decrease from maximum in KO mice was more extreme. Conceivably, the size of myenteric neurons might shrink in an age-related manner that is greater in KO than WT mice. Alternatively, the decrease in the average of Feret's diameters might reflect a differential survival of neurons with larger neurons being lost in preference to smaller ones. An analysis of the cumulative frequency distribution of Feret's diameters at 1 and 12 months (Fig. 2*I*) suggests that an age-associated shift of the population toward smaller diameters occurs in both WT and KO mice; however, the shift is more pronounced in KO than in WT animals. Neuronal nitric oxide synthase (nNOS) was demonstrated immunocytochemically to determine whether age and/or the deletion of 5-HT$_4$ receptors exert a preferential effect on a single chemically defined class of neuron. HuC/D immunoreactivity was simultaneously demonstrated to quantify the total number of myenteric neurons (HuC/D = 100% at each age) and thus to allow the proportion of nitrergic neurons to be estimated. Subsets of nitrergic neurons are inhibitory motor neurons, whereas others are myenteric interneurons. The morphology of both has been classified as Dogiel type I (Ward et al., 1992; Takahashi et al., 2000; Vannucchi et al., 2002; Phillips and Powley, 2007). At 1 month of age, the proportion of nNOS-immunoreactive neurons did not differ significantly in WT (40.1 ± 1.4%) and KO (43.6 ± 1.3%) mice; however, at 12 months of age, the proportion of nitrergic neurons declined to 31.4 ± 2.1% in KO animals ($p < 0.001$ vs KO at 1 month) but remained stable in WT mice (39.2 ± 1.8%); therefore, a selective loss of nitrergic neurons occurred over the course of the first year of life in KO mice ($p < 0.05$; KO vs WT at 12 months). The deletion of 5-HT$_4$ receptors thus does not affect all chemically defined populations of enteric neurons equally.

### Stimulation of 5-HT$_4$ receptors promotes neuronal survival *in vitro*

Because the normal maturation-associated increase in relative numbers of myenteric neurons between 1 and 4 months of age does not occur in KO mice, it is possible that 5-HT$_4$ receptors promote enteric neuronal growth. This hypothesis was tested on enteric neurons grown *in vitro*. Crest-derived progenitors of enteric neurons were isolated from E12–E13 fetal mice by immunoselection with antibodies to p75$^{NTR}$ and cultured for 48 h in serum-free media in the absence or presence of either of two 5-HT$_4$ agonists, RS67506 or tegaserod. Enteric neurogenesis occurs at a high rate in these cultures (Gershon and Ratcliffe, 2006). Two agonists that differ in chemical structure were examined to help verify that observed effects are related to their shared 5-HT$_4$ agonism. Additional verification of specificity was obtained by

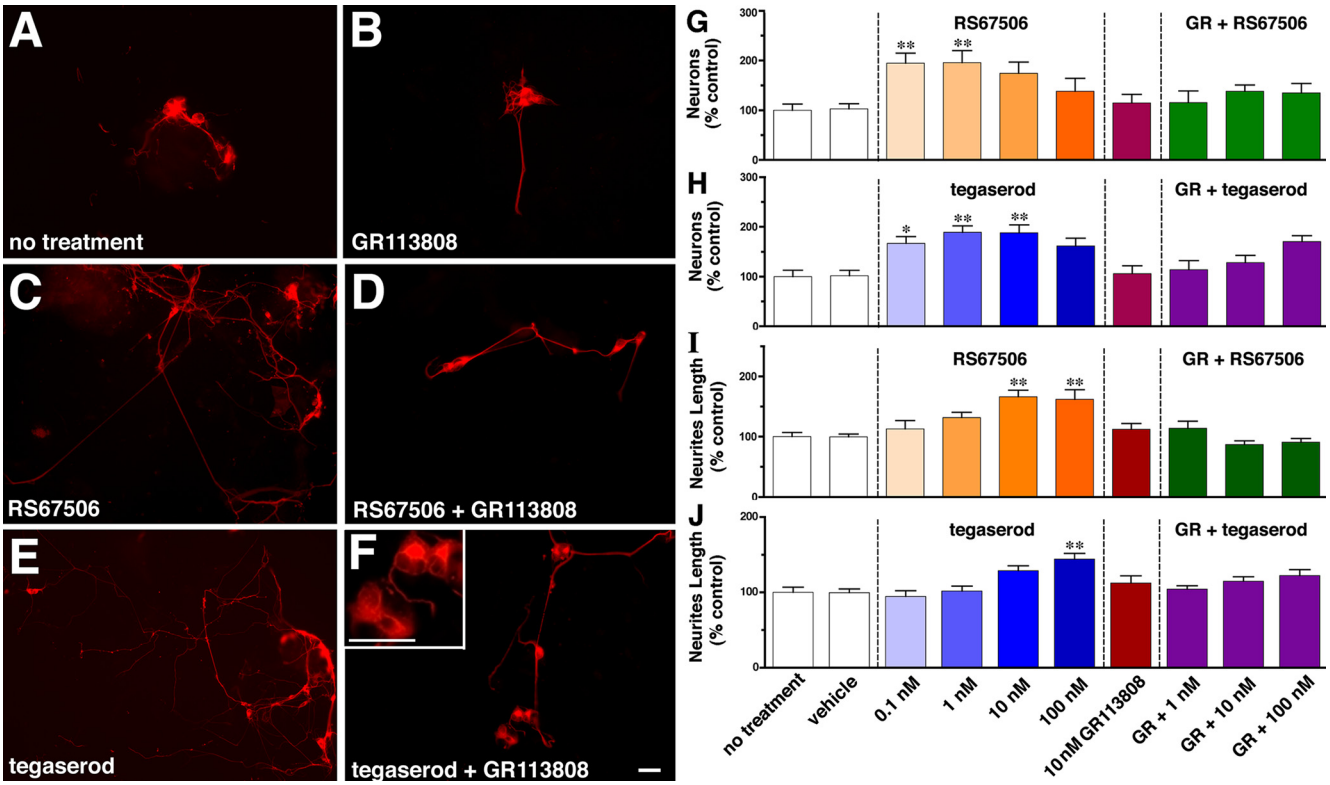


**Figure 3.** 5-HT$_4$ stimulation promotes development/survival and neurite outgrowth in cultures of enteric neurons from fetal mice. Neurons were cultured with either of two 5-HT$_4$ agonists, RS67506 or tegaserod, in the absence or presence of the 5-HT$_4$ antagonist, GR113808. Neurons were identified as β3-tubulin immunoreactive. Numbers of neurons and neurite length were quantified and normalized to control cultures containing no additives. ***A–F***, Representative micrographs. ***A***, No treatment control. ***B***, GR113808. ***C***, RS67506. ***D***, RS67506 plus GR113808. ***E***, Tegaserod. ***F***, Tegaserod plus GR113808. Inset, High-magnification view of a cluster of neurons to illustrate the appearance of cell bodies. Scale bar, 50 μm. ***G***, ***H***, RS67506 (***G***) and tegaserod (***H***) concentration-dependently increased numbers of enteric neurons developing and/or surviving in culture. Although GR113808 had no effect by itself, it blocked effects of RS67506 (***G***) and tegaserod (***H***). ***I***, ***J***, RS67506 (***I***) and tegaserod (***J***) concentration-dependently increased length of neurites. GR113808 had no effect by itself but blocked effects of RS67506 (***I***) and tegaserod (***J***). The DMSO-containing vehicle (***G–J***) exerted no effect. Using immunoselection from fetal mice, which isolated at E12–E13 from total of eight adult female mice, derived four to six cultures of each type. $^*p < 0.05$; $^{**}p < 0.01$ versus no treatment control. Error bars indicate SEM.

determining whether the 5-HT$_4$ antagonist, GR113808, could block agonist effects. Neurons were counted and neurite length was measured in cells identified by the immunocytochemical detection of the neuronal marker, β3-tubulin. Both RS67506 and tegaserod significantly increased the number of neurons developing and/or surviving *in vitro* (Fig. 3*A–H*). The effects of each agonist were concentration dependent; however, at high concentrations of both, promotion of survival/differentiation was lost. Although GR113808 alone had no effect, it blocked RS67506- and tegaserod-enhanced survival/differentiation (Fig. 3*G*,*H*). Both RS67506 and tegaserod also increased neurite length (Fig. 3*I*,*J*), although at higher concentrations than promotion of neuron survival/differentiation. GR113808, which exerted no effect by itself on neurite length, blocked the increase in neurite length in response to RS67506 or tegaserod (Fig. 3*I*,*J*).

When 5-HT$_4$ agonists are added to cultures of precursors immunoselected from fetal bowel, they could conceivably increase neuronal numbers either by enhancing survival, neurogenesis, or both. To determine whether 5-HT$_4$ agonists are neuroprotective, we determined the effect of 5-HT$_4$ agonists on apoptosis of neurons *in vitro*. Apoptosis was demonstrated by using TUNEL assay; enteric neurons were simultaneously visualized with antibodies to β3-tubulin and DNA was stained bisbenzimide (Fig. 4*A–D*). Both RS67506 (Fig. 4*E*) and tegaserod (Fig. 4*F*) at 10 nM decreased the proportion of apoptotic cells ($p < 0.01$). The response to each agonist was concentration dependent and abolished by a selective 5-HT$_4$ antagonist, GR113808, which exerted no significant effects by itself (Fig. 4*E*,*F*). Because the generation of substantial numbers of enteric neurons ceases after P21 (Pham et al., 1991), studies were performed with enteric neurons isolated from adult mice (6–8 weeks of age). Apoptosis was again demonstrated by using the TUNEL method in preparations in which neurons were simultaneously visualized with antibodies to β3-tubulin and DNA was stained with bisbenzimide (Fig. 4*G–J*). RS67506 and tegaserod (10 nM) significantly decreased the proportion of cells undergoing apoptosis ($p < 0.01$) (Fig. 4*K*). The selective 5-HT$_4$ antagonist, SB204070 (10 nM), which by itself did not significantly affect apoptosis, blocked the antiapoptotic response of each 5-HT$_4$ agonist (Fig. 4*K*). Two different 5-HT$_4$ antagonists, GR113808 and SB204070, thus both block the antiapoptotic actions of 5-HT$_4$ agonists. The effects of these antagonists on 5-HT$_4$-dependent whole-cell currents in myenteric neurons have been shown to be equivalent (Liu et al., 2005). These observations, therefore, are consistent with the idea that 5-HT$_4$ agonists are neuroprotective.

### Stimulation of 5-HT$_4$ receptors promotes CREB phosphorylation *in vitro*

5-HT$_4$ receptors are known to be coupled to Gs and to signal by activating adenylyl cyclase to increase cAMP, which activates protein kinase A (PKA) (Dumuis et al., 1989b, 1991; Torres et al., 1995). It is thus possible that CREB, which undergoes nuclear translocation after it has been phosphorylated by PKA (Montminy, 1997; Viola et al., 2000), mediates 5-HT$_4$-associated neuroprotection. pCREB has been reported to be important in

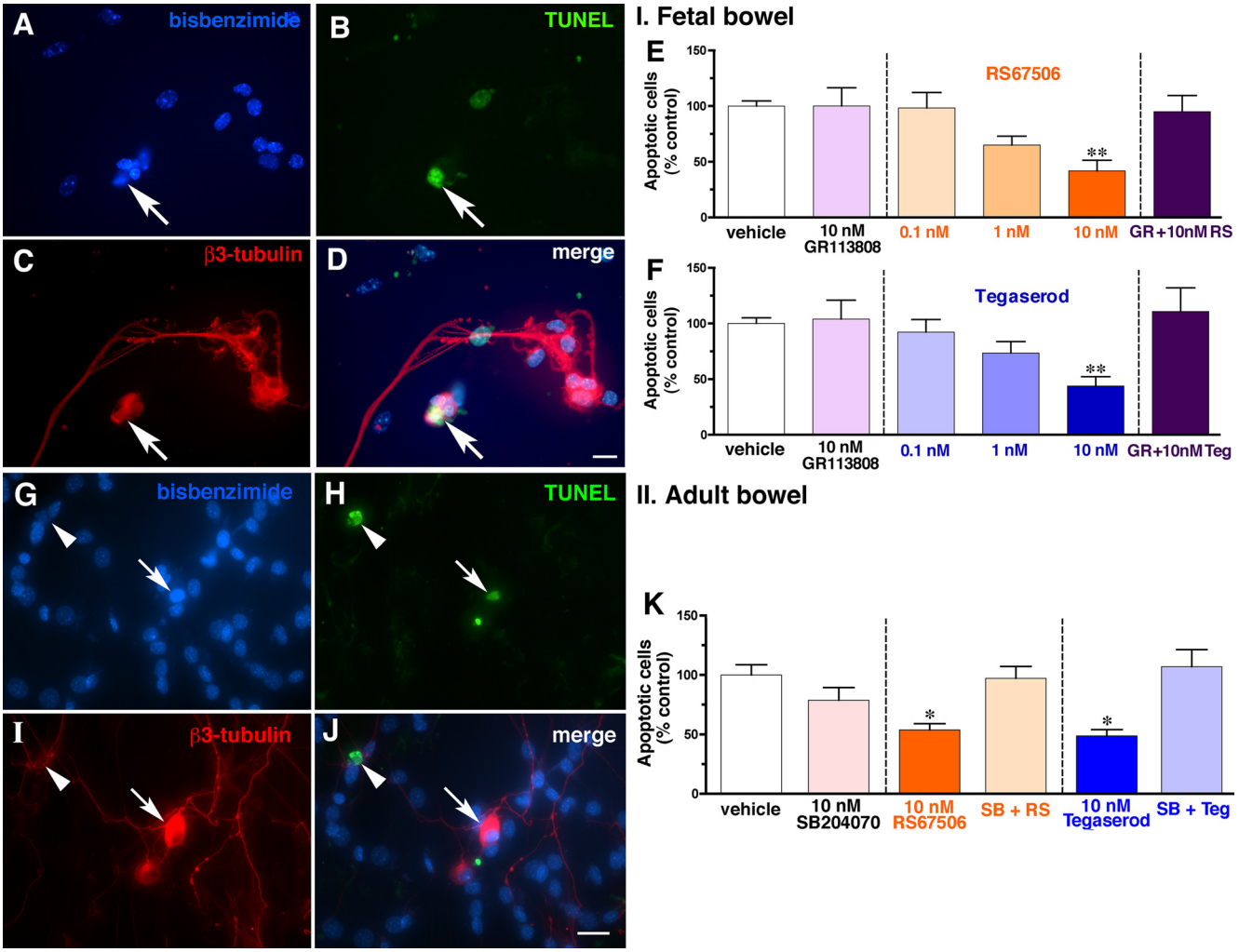


**Figure 4.** Stimulation of 5-HT$_4$ receptors promotes survival of enteric neurons. ***A–F***, Fetal mice: 5-HT$_4$ agonists applied to cultures of enteric neurons developing *in vitro* from crest-derived precursors immunoselected. ***A***, DNA stained with bisbenzimide. ***B***, Apoptosis demonstrated by TUNEL assay. ***C***, Enteric neurons visualized with antibodies to $\beta$3-tubulin. ***D***, Merged image. The arrow points to a neuron undergoing apoptosis. Scale bar, 16 $\mu$m. ***E***, ***F***, The numbers of apoptotic neurons were quantified in cultures exposed to DMSO (vehicle control), either of two 5-HT$_4$ agonists (RS67506 or tegaserod), in the absence or presence of the 5-HT$_4$ antagonist, GR113808. Data were normalized to the vehicle control. Both RS67506 (***E***) and tegaserod (***F***) decreased apoptosis (**$p <$ 0.01 vs control at 10 nM). The effect of each was abolished by GR113808. GR113808 exerted no effect of its own. Using immunoselection from fetal mice, which isolated at E12–E13 from total of six adult female mice, derived three to six cultures of each type. ***G–K***, Adult mice: 5-HT$_4$ agonists applied to cultures of isolated myenteric neurons. ***G***, DNA stained with bisbenzimide. ***H***, Apoptosis demonstrated by TUNEL assay. ***I***, Enteric neurons visualized with antibodies to $\beta$3-tubulin. ***J***, Merged image. The arrow and arrowhead point to neurons in different stages of apoptosis. Scale bar, 20 $\mu$m. ***K***, The numbers of apoptotic neurons were quantified in cultures exposed to DMSO (vehicle control), either of two 5-HT$_4$ agonists (RS67506 or tegaserod), in the absence or presence of the 5-HT$_4$ antagonist, SB204070. Data were normalized to the vehicle control. SB204070 exerted no effect of its own (left panel). Both RS67506 (middle panel) and tegaserod (right panel) decreased apoptosis (*$p <$ 0.01 vs control at 10 nM). The effect of each was abolished by SB204070. The number of mice was six. The number of cultures per treatment was three to six. Error bars indicate SEM.

neuroprotection in the CNS (Bito et al., 1996; Deisseroth et al., 1996; Bito and Takemoto-Kimura, 2003; Lucas et al., 2007). We therefore determined whether stimulation of 5-HT$_4$ receptors causes the nuclear translocation of pCREB in cultured enteric neurons.

Neurons were isolated from adult LMMP (isolated at 6–8 weeks of age), cultured, and exposed for 20 min to RS67506 or tegaserod in the absence or presence of the 5-HT$_4$ antagonist, SB204070, or the PKA inhibitor, H89. Controls included cultures exposed only to vehicle (DMSO), only to SB204070, or only to H89. Immunocytochemistry was used to visualize the nuclear translocation of pCREB and in-cell ELISA was used to quantify pCREB immunoreactivity, which was expressed as the pCREB/CREB ratio (normalized to that observed in vehicle-treated cultures). Neurons were identified with antibodies to the heavy subunit of the neurofilament triplet (NF-H). Little pCREB immunoreactivity was visualized in neurons cultured with vehicle (Fig. 5*A*) or with SB204070 alone (Fig. 5*B*). In contrast, intense nuclear pCREB immunoreactivity was seen in cultures exposed to RS67506 (Fig. 5*C*) or tegaserod (Fig. 5*D*). Both RS67506 (Fig. 5*E*) and tegaserod (Fig. 5*F*), furthermore, increased the pCREB/CREB ratio over that seen in the presence only of vehicle, SB204070, or H89 ( $p < 0.05$) (Fig. 5*E*,*F*). SB204070 (10 nM) and H89 (100 nM) both blocked the RS67506- and the tegaserod-stimulated increase in the pCREB/CREB ratio ( $p < 0.01$) (Fig. 5*E*,*F*). These observations are consistent with the idea that activation of PKA and pCREB mediate 5-HT$_4$-promoted enteric neuronal survival.

### 5-HT$_4$ agonists promote neurogenesis in adult mice

To detect the generation of new enteric neurons in adult mice, BrdU was infused continuously for 7 d by means of an osmotic minipump, which was implanted into the peritoneal cavity of adult male mice at the age of 6 weeks at least. The continuous

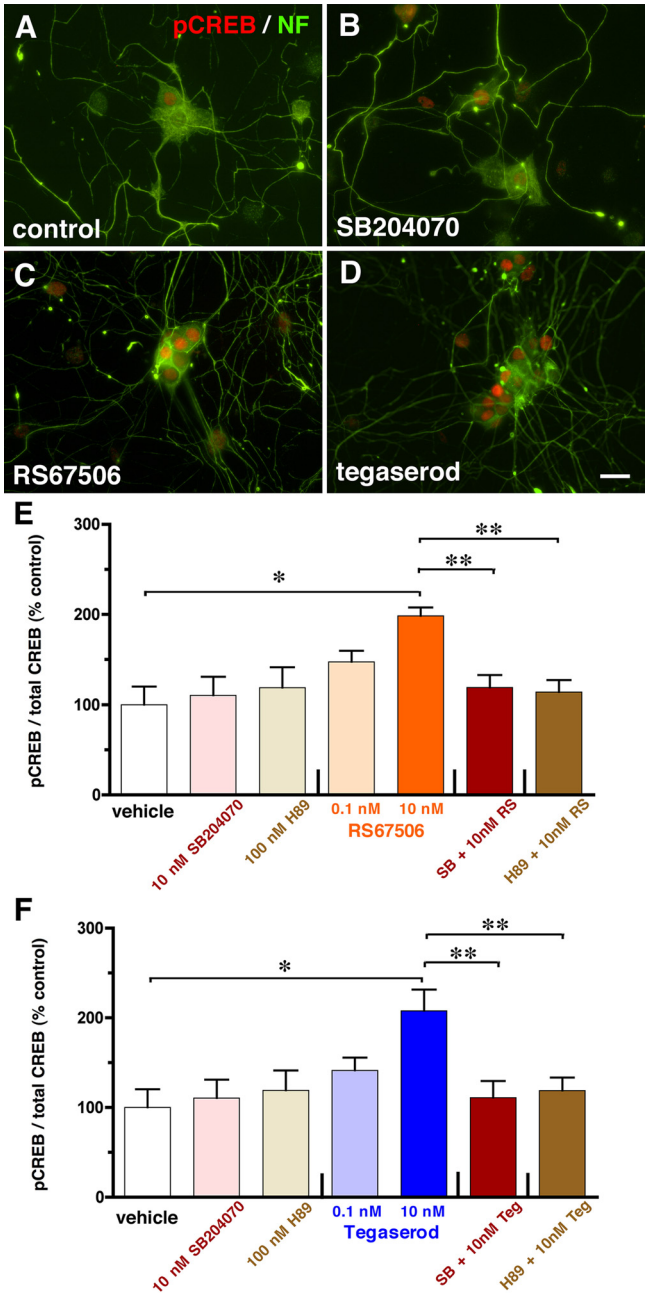


**Figure 5.** Stimulation of 5-HT$_4$ receptors activates CREB in cultures of myenteric neurons isolated from adult mice. Neurons were cultured with either of two 5-HT$_4$ agonists, RS67506 or tegaserod, in the absence or presence of the 5-HT$_4$ antagonist, SB204070. Neurons were demonstrated with antibodies to the heavy subunit of the neurofilament triplet (green), and pCREB immunoreactivity (red). ***A–D***, Immunocytochemistry: Representative micrographs. ***A***, Vehicle control (DMSO). ***B***, SB204070. ***C***, RS67506. ***D***, Tegaserod. Scale bar, 20 $\mu$m. ***E***, ***F***, In-cell ELISA: pCREB and total CREB immunoreactivities quantified in myenteric neurons isolated from adult mice. Both RS67506 (***E***) and tegaserod (***F***) increased the pCREB/total CREB ratio significantly at 10 nM. SB204070 (10 nM) or a PKA inhibitor, H89 (100 nM), blocked the response to both agonists. Neither SB204070 nor H89 affected the pCREB/total CREB ratio when applied individually. Data were normalized to the vehicle control. The number of mice was six. The number of cultures per treatment was three to six. *$p < 0.05$; **$p < 0.01$ versus vehicle control. Error bars indicate SEM.

infusion was used to allow BrdU to be incorporated into the DNA of enteric neuronal precursor cells, even if they infrequently undergo a terminal mitosis. The infusion was followed by a varying periods of chase to allow dividing cells to dilute BrdU and dissipate labeling (Miller and Nowakowski, 1988; del Rio and Soriano, 1989; Nowakowski et al., 1989; Wojtowicz and Kee, 2006; Taupin, 2007). Whole mounts were examined immediately after BrdU infusion and then after intervals of chase (Fig. 6*A*). To determine whether 5-HT$_4$ receptors promote neurogenesis, a 5-HT$_4$ agonist, either RS67506 or tegaserod, was infused together with BrdU for 7 d and were also included in the drinking water during the chase. Control groups (KO mice and their WT littermates) were evaluated with vehicle in the absence of a 5-HT$_4$ agonist in the osmotic minipump and drinking water. DNA was demonstrated with bisbenzimide (bis), and BrdU-labeled cells were immunocytochemically identified with type-specific markers.

Immediately after BrdU infusion (Fig. 6*A*), only a small number of BrdU-labeled cells were detected inside myenteric ganglia in WT mice (Fig. 6*B*). BrdU immunoreactivity was coincident with bisbenzimide (bis)-stained DNA (Fig. 6*C*) and was found in cells with S100$\beta$ immunoreactivity (Bishop et al., 1985; Young et al., 2003) (Fig. 6*D*). The BrdU-labeled cells, therefore, were enteric glia (Fig. 6*B–E*). At this time, no intraganglionic HuC/D-immunoreactive cells were labeled with BrdU. Often, adjacent glia were BrdU labeled. These "doublets" were probably the daughter cells of a recent mitotic event. After 2 weeks of chase, BrdU-labeled glia were no longer detectable in myenteric ganglia, either in the presence or absence of a 5-HT$_4$ agonist.

After 2–4 weeks of chase, BrdU labeling of cells in a neuronal lineage was detected; this labeling was extraganglionic and 5-HT$_4$ agonist dependent (Fig. 7*C–H*). In the absence of a 5-HT$_4$ agonist, virtually no coincident expression of BrdU and HuC/D immunoreactivities was seen in myenteric ganglia after 2 weeks of chase (Fig. 7*A*); moreover, 5-HT$_4$ agonists failed to stimulate the incorporation of BrdU into HuC/D-expressing cells inside or outside of ganglia in KO mice (Fig. 7*B*). In contrast, in WT animals, 5-HT$_4$ agonists did, in fact, stimulate the incorporation of BrdU into small cells that displayed prominent punctate HuC/D immunoreactivity (Fig. 7*C–F*). These BrdU-labeled HuC/D-immunoreactive cells occurred in animals treated either with RS67506 (Fig. 7*C–E*) or tegaserod (Fig. 7*F*) and were found in extraganglionic clusters [visualized on focal planes that differed from those of myenteric ganglia (Fig. 7*E*)]. These doubly labeled extraganglionic cells were encountered in both small (Fig. 7*C*,*E*) and large intestine (Fig. 7*D*,*F*). The punctate nature of the HuC/D-expressing extraganglionic BrdU-labeled cells was different from that of the mature neurons in myenteric ganglia. Because they expressed the neural marker, HuC/D, the BrdU-labeled cells were tentatively identified as neuronal progenitors; thus, the extraganglionic regions in which they were located were called "germinal niches." These niches were located between myenteric ganglia that visualized by the PGP9.5 immunostaining of mature neurons (Wilkinson et al., 1989) (Fig. 7*G*,*H*) and the longitudinal muscle. To locate germinal niches more precisely, a three-dimensional *z*-stack of images was obtained and subjected to deconvolution (see supplemental figures and movies, available at www.jneurosci.org as supplemental material). The vertical distance from the edge of BrdU-labeled cells in a germinal niche to the closest neurons in an adjacent myenteric ganglion was 10–15 $\mu$m after 2 weeks of chase.

Experiments were performed to test the idea that the BrdU-labeled cells in germinal niches were neuronal progenitors. One type of experiment was to determine whether, as in the CNS, the newly generated BrdU-labeled cells expressed the microtubule-associated protein, doublecortin (DCX) (Fig. 7*G*,*H*). In the CNS, DCX is a transient marker of newly generated neurons that are migrating to their final destination (Francis et al., 1999; Gleeson

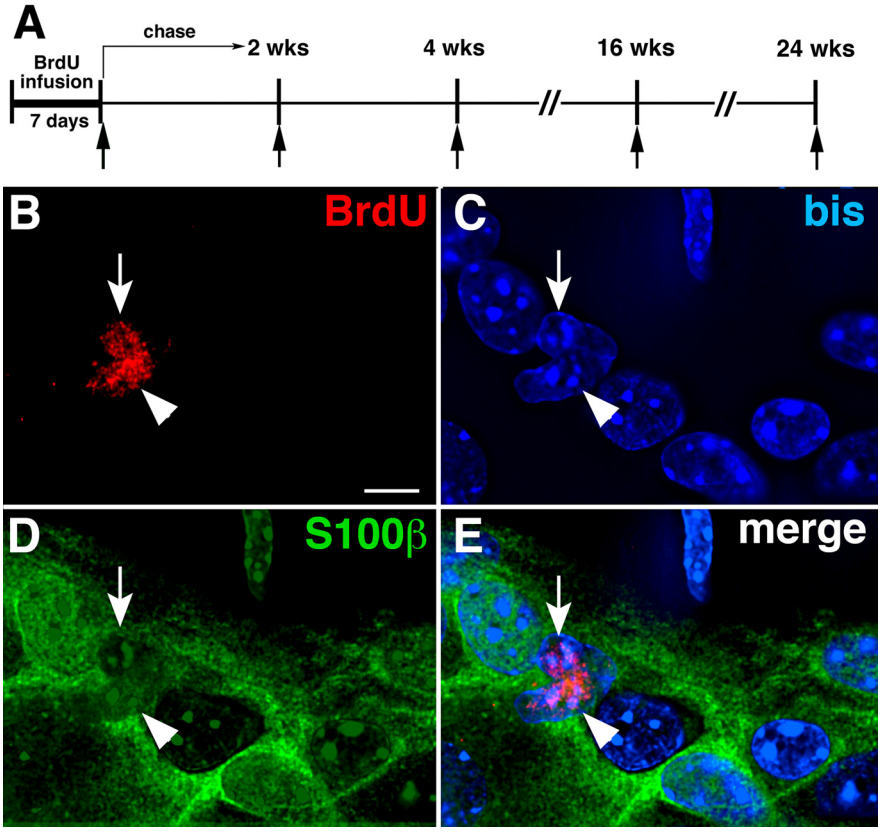


**Figure 6.** BrdU is incorporated into nuclei of glia when myenteric ganglia are examined in the absence of chase (immediately after BrdU infusion). ***A***, A diagram showing the timing of BrdU administration (applies to all subsequent figures). BrdU was infused for 7 d in the presence or absence of 5-HT$_4$ agonists and subsequently subjected to periods of chase that ranged from 0 to 6 months. The arrows indicate the times at which animals were killed for analysis. ***B–E***, BrdU incorporation was examined in the absence of chase (immediately after BrdU infusion). A three-color *Z*-stack of images was obtained by using deconvolution microscopy. The plane illustrated passes through the level with maximal BrdU immunoreactivity. ***B***, BrdU-labeled nuclei (arrow and arrowhead) in myenteric ganglia. ***C***, DNA stained with bisbenzimide (bis) (the arrow and arrowhead point to the nuclei that incorporated BrdU). ***D***, S100$\beta$ immunoreactivity marking enteric glia (the arrow and arrowhead point to the nuclei that incorporated BrdU). ***E***, Merged image (the arrow and arrowhead point to glia that incorporated BrdU). Scale bar, 6 $\mu$m.

et al., 1999; Horesh et al., 1999; Rao and Shetty, 2004; Magavi and Macklis, 2008; Wang et al., 2008). DCX is downregulated in the CNS when migrants mature in their final destinations. The other type of experiment was to determine the position of HuC/D-BrdU-colabeled cells as a function of time of chase after BrdU infusion. If the HuC/D-BrdU-colabeled cells were neuronal progenitors that migrate into myenteric ganglia from their site of generation in germinal niches, they might, like their CNS counterparts, be DCX-immunoreactive, the distance between these cells and myenteric ganglia would be an inverse function of the time of chase, and the cells would eventually enter ganglia. BrdU-labeled cells in germinal niches were labeled with antibodies to DCX after 4 weeks of chase (Fig. 7*G*,*H*).

After 4 weeks of chase (Fig. 8*B*; supplemental Fig. 1, available at www.jneurosci.org as supplemental material), the small HuC/D-BrdU-colabeled cells appeared to be located closer to myenteric ganglia than at 2 weeks (Fig. 7*C*,*D*); however, analyses of *z*-stacks of sequential optical sections revealed that they were still extraganglionic from 4 to 16 weeks (Fig. 8*A–C*; supplemental Figs. 1, 2 and movies 1, 2, available at www.jneurosci.org as supplemental material). The optical plane containing a germinal niche (Fig. 8*A*, left panel) was thus below that of the nearest myenteric ganglion (Fig. 8*A*, right panel). After 16 weeks of chase (Fig. 8*C*; supplemental Fig. 2, available at www.jneurosci.org as supplemental material), the HuC/D-BrdU-colabeled cells were closely apposed to myenteric ganglia, sometimes within their sheath. By 24 weeks of chase, HuC/D-BrdU-colabeled neurons finally were detected within myenteric ganglia (Fig. 8*D*; supplemental Fig. 3, available at www.jneurosci.org as supplemental material). These data are consistent with the idea that myenteric neurons are generated in specialized germinal niches and then migrate slowly toward ganglia, which they enter between 16 and 24 weeks after their birth. The observations suggest that newly generated neurons are small when they insert into ganglia (Fig. 8*D*).

It is noteworthy that, in contrast to the situation that immediately followed BrdU infusion, after 2 weeks of chase, no evidence of BrdU incorporation into glia was obtained, even when animals were exposed to 5-HT agonists (RS67506 or tegaserod) up to 10 weeks. After 4 weeks of chase, glial markers examined for possible colocalization with BrdU included brain fatty acid binding protein (B-FABP) (Fig. 9*A*) (Kurtz et al., 1994; Schnütgen et al., 1996; Young et al., 1996; Young et al., 2003), glial fibrillary acidic protein (GFAP) (Fig. 9*B*) (Jessen and Mirsky, 1980, 1985), and S100$\beta$ (Fig. 9*C*). In mice, 5-HT$_4$ receptors have been detected in enteric neurons and interstitial cells of Cajal but not in glial cells (Liu et al., 2005; Poole et al., 2006); therefore, enteric glia are not responsive to 5-HT$_4$ agonists. It seems more likely, however, that the absence of glial labeling with BrdU is attributable to the rapid rate of enteric glial turnover; even without apparent injury, enteric glia behave like reactive astrocytes (Bush et al., 1998, 1999; Bush, 2002). The dilution of BrdU in glia, which continues to divide during the chase period, thus probably eliminates their labeling.

In contrast to glia, 5-HT$_4$ agonists induced the BrdU labeling of cell germinal niches that displayed the immunoreactivities of transcription factors/intermediate filament proteins that mark crest-derived precursors during gut development, including Sox10 (Fig. 9*D*,*E*$_2$) (Herbarth et al., 1998; Southard-Smith et al., 1998; Maka et al., 2005), Phox2b (Fig. 9*E*$_1$,*E*$_2$) (Pattyn et al., 1999), and nestin (Fig. 9*F*$_1$,*F*$_2$) (Steinert et al., 1999; Chou et al., 2003). The antibodies to Sox10 do not cross-react with the related Sox8 or Sox9, which also appear in developing ENS precursors (Stolt et al., 2003; Maka et al., 2005). The distribution of BrdU-labeled cells was irregular, sparse, and extraganglionic, making it difficult to quantify cells that coexpressed HuC/D (Fig. 9*D*,*E*$_1$,*F*,*G*), Sox10 (Fig. 9*D*), Phox2b (Fig. 9*E*$_1$), or nestin (Fig. 9*F*$_1$,*F*$_2$) with BrdU. The germinal niches in which BrdU/Hu-immunoreactive cells were sometimes relatively numerous, were often close to ganglia, but below them, between a ganglion and the longitudinal muscle after 4 weeks of chase (Fig. 9*G*).

A subset of cells that incorporated BrdU after RS67506 stimulation of 5-HT$_4$ receptors and 4 weeks of chase was Musashi-1 (Msi1)-immunoreactive (Fig. 9*H*). Msi1 is a marker for stem

cells in the fetal and adult CNS and intestinal epithelium (Nagata et al., 1999; Kaneko et al., 2000; Nishimura et al., 2003; Potten et al., 2003; Fukui et al., 2006). Although epithelial Msi1-labeled cells have been detected with immunocytochemistry and *in situ* hybridization in mouse intestinal epithelial crypts and serosa (Potten et al., 2003; May et al., 2008), this is the first report of Msi1-immunoreactive cells associated with the ENS. The cells with coincident BrdU and Msi1 labeling were adjacent to myenteric ganglia and near HuC/D-immunoreactive cells (Fig. 9*H*). Rarely, punctate perinuclear HuC/D immunoreactivity could be detected in BrdU-labeled Msi1-immunoreactive cells (Fig. 9*H*). The appearance of these rare triply labeled cells is consistent with the possibility that Msi1-immunoreactive stem cells that incorporated BrdU during a terminal mitosis were fixed while in transition to becoming HuC/D-immunoreactive neurons. Because Msi1 immunoreacvtivity in the intestine has previously been located mostly in the mucosa, immunoblots were performed to verify antibody specificity. Tissue lysates were derived from mechanically isolated preparations of intestinal mucosa, LMMP, and hippocampus (Fig. 9*I*). Antibodies to $\alpha$-tubulin were used as loading control. A size-appropriate ~39 kDa Msi1-immunoreactive band was found in all three preparations; relatively, more Msi1 immunoreactivity was detected in the intestinal mucosa than in either the LMMP or hippocampus. The extraganglionic locations of BrdU-labeled cells that coexpress Msi1 and/or markers of ENS precursors and the time-dependent translocation of BrdU-labeled neurons into ganglia fit the model shown diagrammatically in Figure 9*J*.

To verify that uptake of BrdU was 5-HT$_4$ dependent, experiments were performed in LMMP preparations from KO mice and their WT littermates after 4 weeks of chase, and BrdU incorporation was quantified by using in-cell ELISA (Fig. 9*K*). The administration of DMSO/saline was used as a vehicle control. Treatment of WT mice with RS67506 or tegaserod significantly increased BrdU incorporation ($p < 0.01$) (Fig. 9*K*, left panel). In contrast, neither RS67506 nor tegaserod was able to increase BrdU incorporation in KO mice ($p < 0.01$) (Fig. 9*K*, right panel). In fact, tegaserod, which is a 5-HT$_{2B}$ antagonist as well as a 5-HT$_4$ agonist (Beattie et al., 2004), reduced the incorporation of BrdU to a level that was significantly below that seen in control KO mice. 5-HT$_{2B}$ antagonism in tegaserod may be responsible for this effect; 5-HT$_{2B}$ receptors have been demonstrated in fetal bowel to promote neurogenesis, and, although down-regulated, they are retained in the adult ENS (Fiorica-Howells et al., 2000).

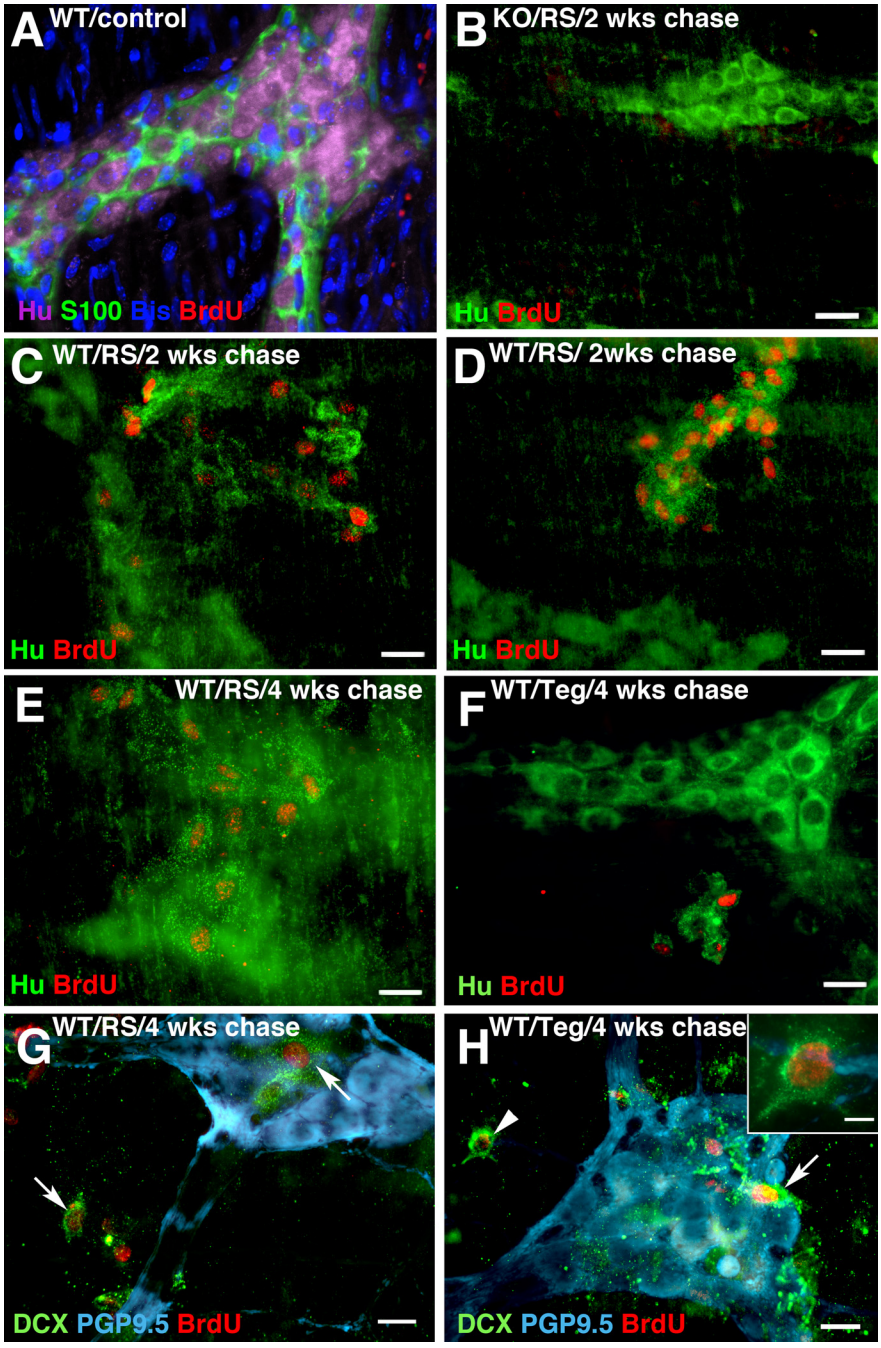


**Figure 7.** 5-HT$_4$ agonists promote neurogenesis in germinal niches in adult mouse gut. BrdU-labeled cells in a neuronal lineage were identified with antibodies to HuC/D. ***A***, WT mouse, no exposure to 5-HT$_4$ agonists, 2 weeks chase. No neurons (HuC/D) or glia (S100$\beta$) labeled with BrdU. DNA stained with bis. Scale bar, 20 $\mu$m. ***B***, KO mouse, RS67506-treated, 2 weeks chase. No neurons (HuC/D) were labeled with BrdU. Scale bar, 16 $\mu$m. ***C***, ***D***, WT mice, exposed to 5-HT$_4$ agonists, 2 weeks chase. Cells in clusters (germinal niches) adjacent to myenteric ganglia display coincident labeling with BrdU and punctate HuC/D. ***C***, Ileum/RS67506. ***D***, Colon/RS67506. Scale bar, 16 $\mu$m. ***E***, ***F***, WT mice, exposed to 5-HT$_4$ agonists, 4 weeks chase. BrdU-labeled nuclei are present in extraganglionic cells with punctate HuC/D immunoreactivity (germinal niches). ***E***, Ileum/RS67506. ***F***, Colon/tegaserod. Scale bar, 16 $\mu$m. ***G***, ***H***, WT mice, colon, 5-HT$_4$ agonists, 4 weeks chase. BrdU was incorporated into the nuclei of extraganglionic cells that were coimmunostained with the early neural marker DCX (arrows and arrowhead). Myenteric ganglia are identified by their immunostaining with antibodies to the neuronal marker, PGP9.5. The BrdU/DCX-colabeled cells are not in the same focal plane as the myenteric ganglia that are PGP9.5 immunoreactive. ***G***, RS67506. ***H***, Tegaserod. An extraganglionic DCX-immunoreactive cell that incorporated BrdU (arrowhead) is shown at higher magnification in the inset in ***H***. Scale bars: ***G***, ***H***, 20 $\mu$m; ***H***, inset, 6 $\mu$m.

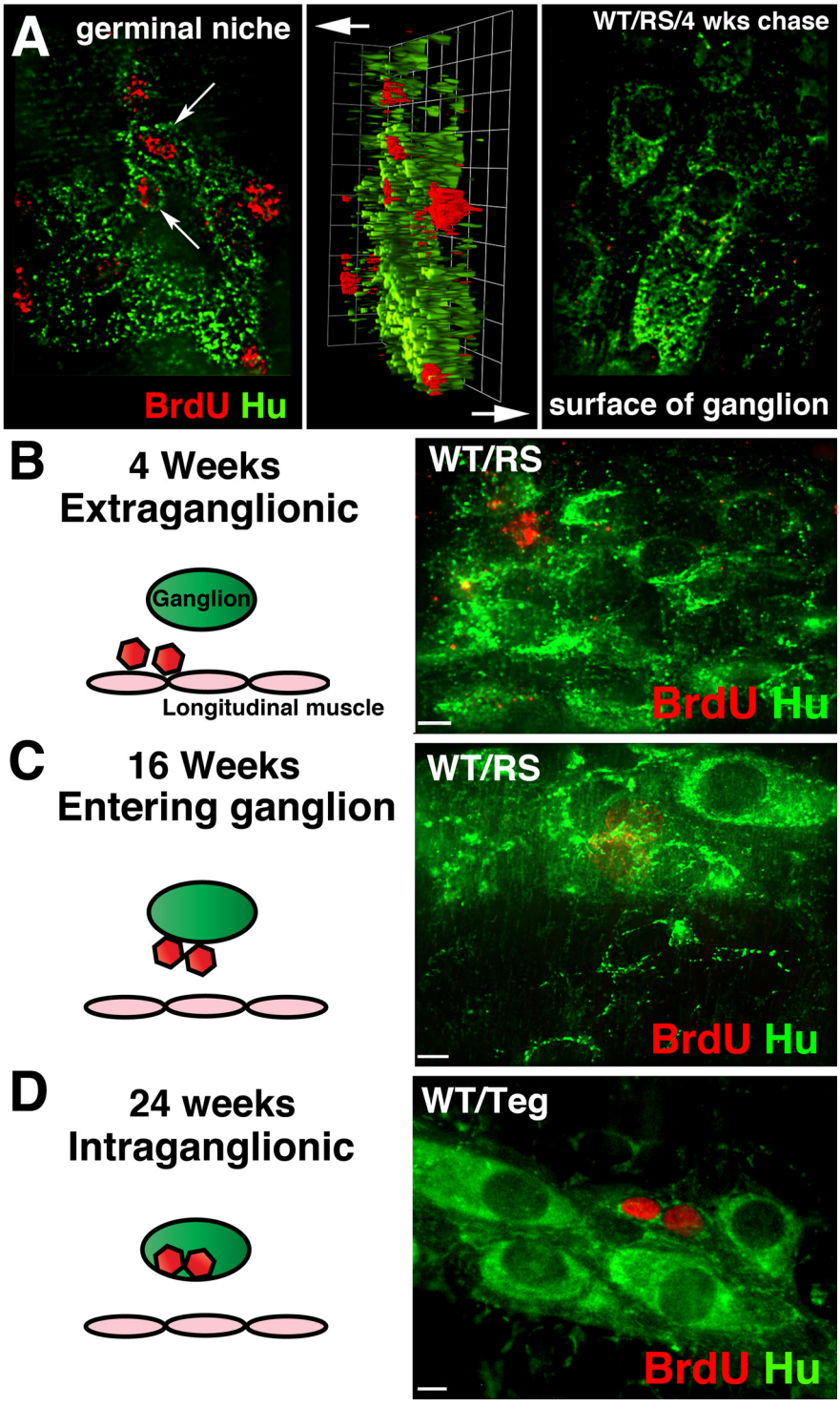


**Figure 8.** The location of BrdU-labeled HuC/D-immunoreactive cells was studied by analyzing *z*-stacks of deconvoluted images through LMMP preparations of WT mouse colon at 4, 16, and 24 weeks of chase. 5-HT$_4$ receptors were stimulated with RS67506 (***A–C***) or tegaserod (***D***). The immunoreactivity HuC/D (green) was used as a neuronal marker and that of BrdU (red) was used to mark cells undergoing mitosis during the pulse of BrdU. ***A***, Four weeks of chase. Cells that are doubly labeled with antibodies to HuC/D and BrdU are still extraganglionic. The center panel shows a rotated image of the three-dimensional stack to provide a lateral view (1 unit = 8.2 $\mu$m); the panel at the left shows a focal plane imaged close to the level of the longitudinal muscle and the panel at the right illustrates a focal plane through the lower surface of a myenteric ganglion, which contains characteristic HuC/D-immunoreactive mature neurons that are not labeled with BrdU. The germinal niche is extraganglionic and located well below the ganglion. ***B–D***, The diagrams at the left show the location of newly generated neuroblasts (cells that are colabeled with antibodies to BrdU and HuC/D; red hexagons), in relation to the longitudinal muscle (mauve ovals) and the nearest myenteric ganglion (green oval). The corresponding projection images from three-dimensional stack viewed vertically are illustrated to the right of the diagrams. ***B***, Four weeks of chase. ***C***, Sixteen weeks of chase. ***D***, Twenty-four weeks of chase. Between 4 and 16 weeks, the newly generated neuroblasts moved closer to a ganglion, but newly generated neurons were not found in a ganglion until 24 weeks of chase. Scale bar, 6 $\mu$m.

### Cell proliferation is attenuated and autophagy is prominent in the ENS of KO mice

The observations that BrdU is incorporated into cells that develop as small neurons in myenteric ganglia and that relative neuronal numbers increase in WT mice between 4 and 16 weeks suggest that myenteric neuronal progenitors divide constitutively at a slow rate. These dividing cells would be expected to be located in germinal niches rather than in ganglia. Ki67 immunoreactivity marks cells capable of mitosis (Key et al., 1994) and thus was used to detect such cells in LMMP. Small numbers of Ki67-immunoreactive cells were detected in control LMMP (Fig. 10*A*); some of these cells were nonneuronal, but others, all extraganglionic; some displayed punctate HuC/D immunoreactivity. Almost no such extraganglionic Ki67-labeled cells were observed in KO mice (Fig. 10*B*). The total number of Ki67-immunoreactive cells in KO mice was only 28.1 $\pm$ 5.3% of that found in WT animals ( $p < 0.01$; $n = 3$).

Because 5-HT$_4$ agonists enhanced neurite outgrowth *in vitro*, neurites were investigated by immunostaining the myenteric plexus with antibodies to the intermediate filament protein, peripherin (Portier et al., 1983; Baetge et al., 1990; Troy et al., 1990) (Fig. 10*C*,*D*,*D*′). Terminal axons were identified simultaneously with antibodies to the synaptic vesicle protein, synaptotagmin (Kraszewski et al., 1995; Yoshihara et al., 2005). In WT mice, peripherin-immunoreactive neurites were found in ganglia, interganglionic connectives, and the tertiary plexus (Fig. 10*C*). Synaptotagmin-immunoreactive varicosities were abundant in ganglia, uncommon in interganglionic connectives, but numerous in the tertiary plexus, which provides an innervation to the longitudinal muscle (Llewellyn-Smith et al., 1993). All of the synaptotagmin-immunoreactive varicosities in the tertiary plexus and circular muscle were found along the course of intact peripherin-immunoreactive neurites. In KO mice (Fig. 10*D*,*D*′), peripherin-immunoreactive fibers were coarser than in WT, but more strikingly, clusters of peripherin-immunoreactive swellings, which were devoid of synaptotagmin immunoreactivity, were found at the ends of nerve fibers (Fig. 10*D*,*D*′). These swellings looked like bunches of grapes extending from stems and were rare in WT mice (Fig. 10, compare *D*, *C*). Because of their morphology and lack of synaptic vesicles, the peripherin-immunoreactive swellings were thought to be swellings (retraction

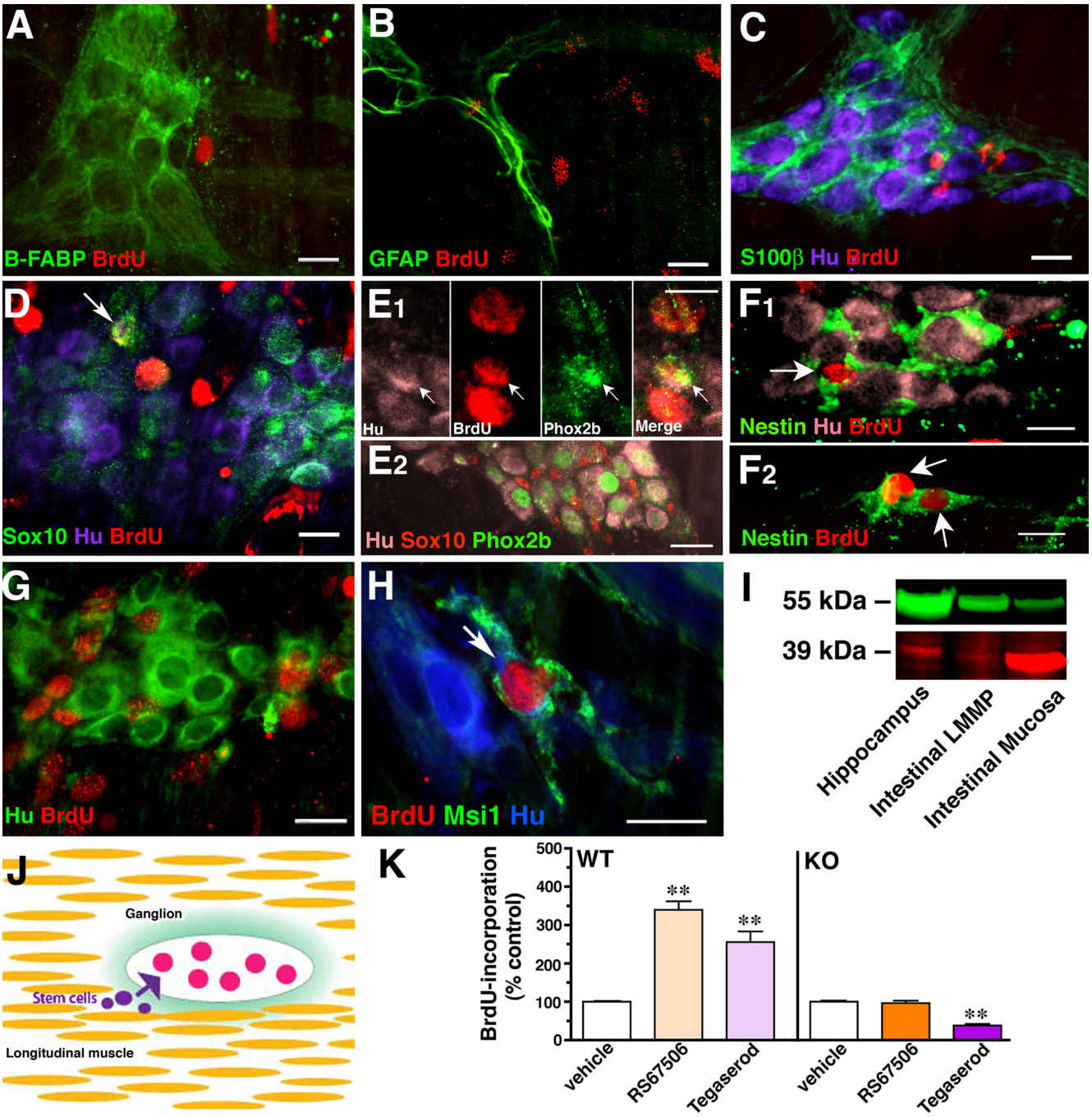


**Figure 9.** Cells that display 5-HT$_4$-induced BrdU incorporation express markers associated with crest-derived progenitors developing in a neuronal lineage. ***A–C***, WT mouse treated with RS67506. After 4 weeks of chase, BrdU is not incorporated by cells that immunostained with antibodies to the glial markers B-FABP (***A***), GFAP (***B***), and S100$\beta$ (***C***). Scale bar, 16 $\mu$m. ***D–F***, WT mice, RS67506-treated. After 4 weeks of chase, BrdU is incorporated into extraganglionic Hu-immunoreactive cells that were labeled with antibodies to Sox10 (***D***, arrow), Phox2b (***E$_1$***, arrow), or nestin (***F$_1$***, arrow). Scale bar, 16 $\mu$m. The position of mature neurons in myenteric ganglia is shown by their HuC/D immunoreactivity. A typical myenteric ganglion is shown in ***E$_2$*** (Hu and Phox2b, myenteric neurons; Sox10, enteric glia). Note that mature neurons in ***C–F*** are intraganglionic and thus located in a focal plane that is different from that of the BrdU-immunoreactive extraganglionic germinal niche cells that coimmunostain with antibodies to HuC/D, Sox10 (***D***), Phox2b (***E$_1$***), or nestin (***F$_1$***, ***F$_2$***). ***G***, In a WT mouse treated with RS67506, the cells that incorporate BrdU are located on a focal plane that is different from that of myenteric neurons labeled with HuC/D after 4 weeks of chase. Scale bar, 16 $\mu$m. ***H***, WT mouse, RS67506-treated, 4 weeks chase. Cells that display 5-HT$_4$-stimulated BrdU incorporation are Msi1 immunoreactive, which are adjacent to myenteric ganglia or near HuC/D-immunoreactive neurons. The Msi1-immunoreactive cell that incorporated BrdU appears to be acquiring perinuclear HuC/D immunoreactivity (arrow). This cell may be in transition from a stem or precursor cell to a progenitor in a neuronal lineage. Scale bar, 16 $\mu$m. ***I***, Immunoblot. Msi1 immunoreactivity (39 kDa) can be detected not only in the intestinal mucosa and hippocampus but also in the intestinal LMMP. Antibodies to $\alpha$-tubulin (55 kDa) were used as loading control. ***J***, Presumed model to explain the extraganglionic location of BrdU-labeled cells that coexpress markers associated with crest-derived neural/glial precursors. Stem cells are located outside of ganglia, in which the terminal mitoses of neuronal precursors occur; progeny committed to a neuronal lineage then slowly migrate into ganglia. ***K***, In-cell ELISA quantitation of BrdU incorporation into myenteric neurons isolated from LMMP of adult mice after 4 weeks of chase. Data are normalized to the vehicle controls for WT and KO mice (white bars). Exposure of WT mice to RS67506 or tegaserod significantly increased BrdU incorporation ( $^{**}p < 0.01$ vs WT). Neither RS67506 nor tegaserod increases BrdU incorporation in KO mice; tegaserod exposure reduced BrdU incorporation in the KO animals ( $^{**}p < 0.01$ vs KO). The number of mice per group was six. Error bars indicate SEM.

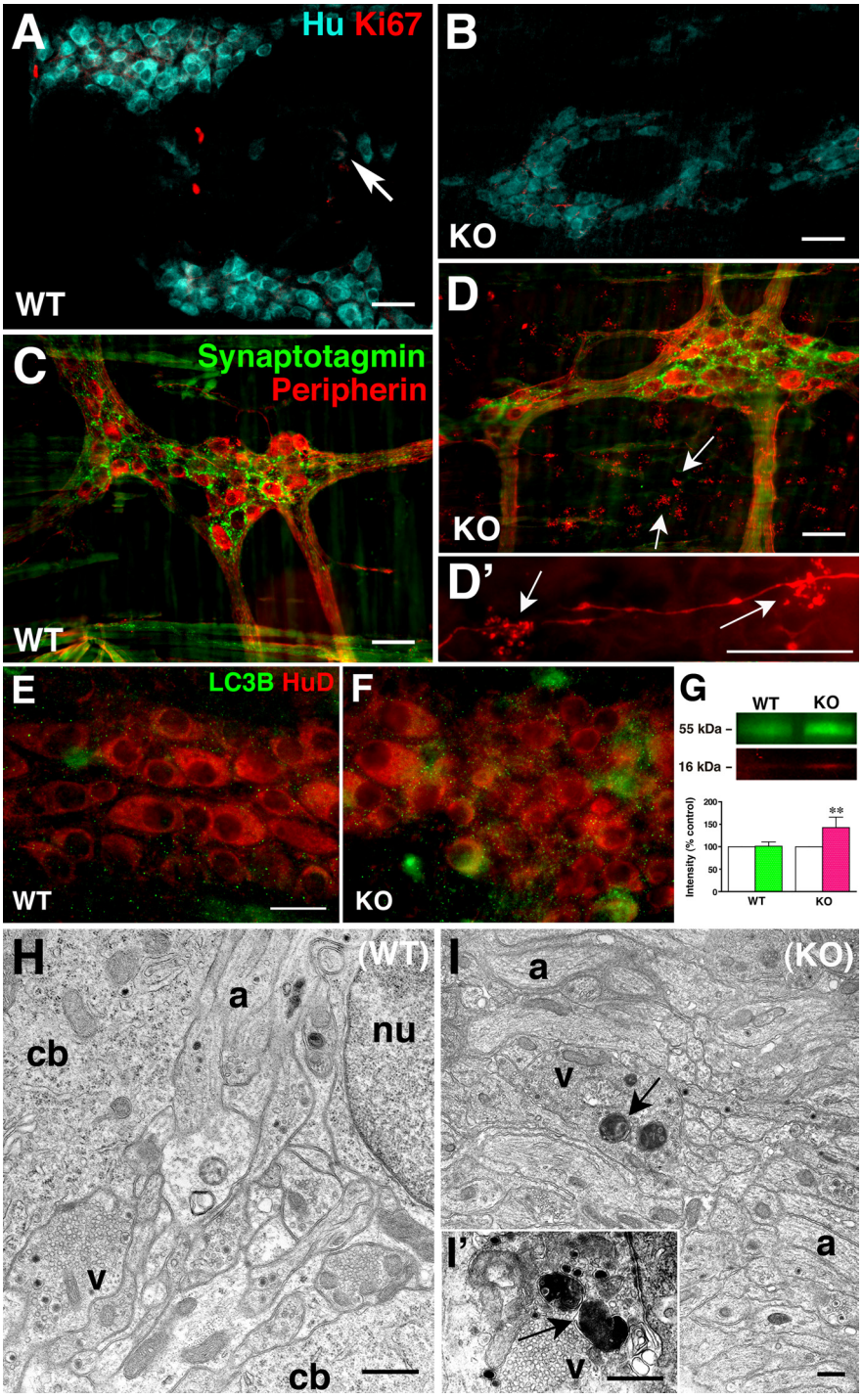


**Figure 10.** Cell proliferation is reduced and autophagy is increased in KO mice. ***A***, ***B***, Proliferating cells were detected with antibodies to Ki67 and neurons with antibodies to HuC/D. ***A***, WT mice. Ki67 labeled nuclei of small extraganglionic clusters of cells with punctate HuC/D immunoreactivity (arrow). ***B***, KO mice. No coincident labeling of cells with Ki67 and HuC/D is seen. Scale bar, 50 $\mu$m. ***C***, ***D***, Synaptotagmin- and peripherin-immunostained LMMP preparations isolated from WT (***C***) and KO (***D***, ***D'***) mice. Peripherin-immunoreactive retraction bulbs (arrows) are found at the ends of neurites in circular muscle, tertiary plexus, and within myenteric ganglia in KO but not in WT mice. The degenerating terminals (retraction bulbs; arrows) extending from intact varicose axons are shown in ***D'***. Many more retraction bulbs were found in LMMP from KO than WT mice. Scale bar, 50 $\mu$m. ***E***, ***F***, The autophagy marker, LC3B, is located immunocytochemically in HuD-expressing neurons and the neuropil of myenteric ganglia in WT (***E***) and KO (***F***) mice. Scale bar, 25 $\mu$m. ***G***, Immunoblot showing LC3B immunoreactivity (16 kDa) extracted from membrane fractions from LMMP preparations of murine colons. The relative intensity of LC3B immunoreactivity was normalized to that of $\alpha$-tubulin (55 kDa). The relative intensity of LC3B immunoreactivity of KO mice is significantly greater than that of WT mice (**$p < 0.01$; $n = 3$). The number of mice per group was three. Error bars indicate SEM. ***H***, ***I***, Electron micrographs of the myenteric plexus of WT (***H***) and KO (***I***) mice. cb, Nerve cell body; a, axon; v, varicosities; nu, nucleus. Autophagy is rare in the ENS of WT (***H***) but prominent in that of KO (***I***) mice. Autophagic structures (arrows) were found in neuronal cell bodies (not illustrated) and in dilated axonal varicosities (***I***, ***I'***). Scale bar, 500 nm.

bulbs) at the viable ends of damaged nerve fibers (Dickson et al., 2007; Ertürk et al., 2007). A small number of retraction bulbs are normally found in LMMP preparations, because the dissection involved in making LMMP preparations damages nerve fibers extending from the myenteric plexus to inner gut layers; however, the numbers of peripherin-immunoreactive retraction bulbs in LMMP preparations from KO mice were significantly greater (141.1 ± 17.9%) than in those of WT mice ($p < 0.01$; $n = 3$). The evidence of constitutive nerve terminal damage in KO mice is consistent with the idea that 5-HT$_4$ receptors contribute to maintenance of myenteric nerve terminals.

Damage or recurrent degeneration of their terminals would be expected to be stressful for myenteric neurons; nevertheless, the TUNEL method failed to reveal apoptotic neurons in these animals (data not shown). It thus seems likely that myenteric neurons are able to survive the damage caused by 5-HT$_4$ depletion. Autophagy can enable neurons to remove damaged cytosol or organelles to survive (Bredesen et al., 2006; Klionsky et al., 2008). To compare the extent of autophagy in WT and KO mice, the marker, microtubule-associated protein 1 light chain 3B (LC3B) (Kabeya et al., 2000; Klionsky et al., 2008) was demonstrated immunocytochemically. Ganglia were also examined by electron microscopy. Little LC3B immunoreactivity was seen in myenteric neurons or the ganglionic neuropil in WT mice (Fig. 10*E*). In contrast, LC3B immunoreactivity was extensive in KO littermates (Fig. 10*F*). A 16 kDa single LC3B immunoreactivity band was found in immunoblots of membrane fractions isolated from LMMP preparations of WT and KO colons (Fig. 10*G*). The relative intensity of LC3B immunoreactivity in KO mice, normalized to $\alpha$-tubulin, was significantly greater than that in WT littermates ($p < 0.01$; $n = 3$) (Fig. 10*G*).

Electron microscopy (EM) was used to confirm the immunocytochemical data suggesting that neurites degenerate and autophagy occurs in the KO mice ENS. Because autophagy is a dynamic and continuous process, many stages of the process are found in electron micrographs, ranging from the earliest sequestering phagophore to the final autophagolysosome, which contains cytoplasmic structures in various stages of digestion (Klionsky et al., 2008). To examine the myenteric plexus, thin sections were cut through flat mounts of colon in the plane of the ganglia. Autophagy was found to be very rare

in the ganglia of WT mice, and when it occurred, autophagic structures were small and limited to restricted regions of the cytoplasm of otherwise normal appearing neurons or neurites (Fig. 10*H*). In contrast, in KO mice, autophagic structures were large, abundant, and most common near synaptic specializations (Fig. 10*I*,*I*′). Changes, which included distention of cisternae of the endoplasmic reticulum, mitochondrial swelling, and the presence of vacuoles in the cytoplasm were also seen in some nerve cell bodies (not illustrated). The extensive autophagy in the ENS of KO mice may be an injury response in which damaged organelles and/or neurons are eliminated; alternatively, autophagic death might account for the loss of neurons that occurs without detectable apoptosis in KO mice.

## Discussion

Neurogenesis is now known to occur throughout life in the subventricular zone (SVZ) of the lateral ventricles and in the subgranular zone of the dentate gyrus of the hippocampus (Zhao et al., 2008). Changes in physiological activity or pathological events can regulate the rate and extent of neurogenesis in both of these regions. After their generation, new neurons migrate to definitive locations, such as the olfactory bulb, which may be quite distant from the site of their birth, in this case, the SVZ. Newly generated neurons, moreover, can integrate into existing brain circuits and receive functional connections. Adult neurogenesis has been much less studied in PNS ganglia than in the brain. Sensory ganglia contain neural crest-derived precursors that can proliferate and give rise to neurons *in vitro* (Li et al., 2007), and *in vivo* neurogenesis is provoked by capsaicin-mediated destruction of existing neurons in rat nodose ganglia (Czaja et al., 2008). In contrast, addition of primary sensory neurons in the adult rat trigeminal ganglion has been reported to occur, not as a result of the terminal mitosis of postnatal precursors, but because of the protracted maturation of postmitotic progenitors (Lagares et al., 2007). In common with other PNS ganglia, the adult ENS contains stem cells that can, *in vitro*, give rise to neurons (Bixby et al., 2002; Kruger et al., 2002; Bondurand et al., 2003; Almond et al., 2007; Estrada-Mondaca et al., 2007; Lindley et al., 2008). Despite the repeated demonstration of precursors in the ENS that are capable of *in vitro* neurogenesis, that process has proven to be difficult to demonstrate *in vivo*.

Neurons are generated in the ENS during the early postnatal period, and injections of $^3$H-dT or BrdU in mice have demonstrated that their birthdays continue through day P21. The ENS, however, continues to enlarge after P21 as the bowel grows in length and diameter, suggesting that neurons continue to be generated (Geuna et al., 2002). Indeed, this process was documented in the current study in which relative enteric neuronal numbers increased in WT mice between 1 and 4 months after birth. This increase evidently occurs at too low a rate to be detected by a single pulse of $^3$H-dT and thus was not seen in the previous study of enteric neuronal birthdays (Pham et al., 1991). That the normal age- and growth-related increase in neurons failed to occur in 5-HT$_4$ KO mice is consistent with the possibility that it is 5-HT$_4$ dependent. Alternatively, it is possible that neuronal numbers fail to increase between 1 and 4 months in 5-HT$_4$ KO mice because they are anorexic and eat poorly (Compan et al., 2004; Jean et al., 2007). Enteric neurons also increase significantly in numbers proximal to intestinal obstructions (Gabella and Trigg, 1984; Geuna et al., 2002). Because this increase occurs in the absence of detectable mitotic figures, obstruction-induced increases in neurons have been attributed to the differentiation of previously dormant postmitotic progenitors.

Several factors explain why neurogenesis might be difficult to demonstrate even though the postnatal ENS retains stem cells. A low rate of neuronal birthdays would be likely to escape detection by a single systemic injection of BrdU because the coincidence of a terminal mitosis occurring during the relatively short period of time that BrdU is circulating and available for uptake would be a rare event. Newly generated neurons, moreover, might arise in specialized locations and migrate into ganglia. If so, the correct sites would have to be examined to enable enteric neurogenesis to be detected. Conceivably, physiological or pathological stimuli that increase enteric neurogenesis might also be needed to facilitate the detection of neurogenesis. To test the hypothesis that neurogenesis occurs in adult bowel, we administered BrdU continually for 7 d to allow newborn neurons to accumulate and we applied a 5-HT$_4$ agonist to increase neurogenesis; in addition, we examined whole mounts of laminar preparations, so as not to miss putative germinal niches should they exist in extraganglionic locations.

Even a long-term administration of BrdU did not, by itself, cause BrdU to be incorporated into enteric neurons. In contrast, exposing the bowel to a 5-HT$_4$ agonist along with long-term BrdU administration induced BrdU to label cells that also expressed markers of cells in a neuronal lineage. These markers included the immunoreactivities of HuC/D, DCX, Sox10, Phox2b, and nestin. The cells that exhibited BrdU and punctate HuC/D immunoreactivity were found in germinal niches between myenteric ganglia and the longitudinal smooth muscle layer. Proximity of BrdU-HuC/D-labeled cells to ganglia was inversely related to the length of chase after BrdU administration; after 24 weeks, they were intraganglionic and appeared to be small neurons. These observations suggest that enteric neurogenesis occurs *in vivo*, but at too low a rate to be detected unless the rate is increased by a stimulus, such as activation of 5-HT$_4$ receptors. Stimulation of 5-HT$_4$ receptors has also been reported to enhance neurogenesis in the CNS (Lucas et al., 2007).

5-HT$_4$ agonist-promoted enteric neurogenesis was probably 5-HT$_4$ receptor specific. Two agonists with different chemical structures, RS67506 and tegaserod, were each effective, and the response was observed in WT but not in KO mice. 5-HT$_4$ receptors, furthermore, are probably significant postnatal regulators of neurogenesis and/or survival because the increase (1–4 months) in the number of enteric neurons that is normally seen during the maturation of the bowel in early life did not occur in KO mice. As a result, the decline in neuronal numbers, which occurred between 4 and 12 months in both WT and KO animals, was more severe in KO mice. These differences could be explained by a deficiency in enteric neurogenesis and/or survival in KO mice. Neither the TUNEL method nor EM, however, was able to detect apoptotic neurons in either WT or KO bowel. In contrast, autophagy was prominent in the ENS of KO mice and substantial numbers of retraction bulbs were found in neurites within the circular muscle, tertiary plexus, and myenteric ganglia. Conceivably, autophagy might help neurons survive damage to distal neurites (Bredesen et al., 2006; Klionsky et al., 2008). In any case, the increased autophagy in KO animals suggests that 5-HT$_4$ receptors contribute to maintenance of the ENS.

To determine whether 5-HT$_4$ receptor stimulation is neuroprotective, enteric neurons from fetal and adult mice were grown *in vitro*. Under culture conditions, many neurons normally undergo apoptosis. 5-HT$_4$ agonists (RS67506 and tegaserod) significantly enhanced neuronal survival and decreased apoptosis. RS67506 and tegaserod also promoted neurite extension *in vitro*. Each of these effects were 5-HT$_4$ specific in that they were blocked

by a 5-$HT_4$ antagonist, GR113808 or SB204070. RS67506 and tegaserod, moreover, each promoted the phosphorylation and nuclear translocation of CREB *in vitro*. The 5-$HT_4$ agonist-induced activation of CREB was also blocked by SB204070 and by the PKA inhibitor, H89, and was thus specific. These effects are consistent with the idea that enteric neuronal 5-$HT_4$ receptors are coupled to Gs, cAMP, PKA, and pCREB (Dumuis et al., 1989b, 1991; Torres et al., 1995; Lambert et al., 2001). pCREB, moreover, has been shown to promote neuronal survival (Nakagawa et al., 2002; Bito and Takemoto-Kimura, 2003). 5-$HT_4$ agonists thus activate PKA- and pCREB-dependent survival pathways in enteric neurons.

Gastric emptying and intestinal motility were slower in KO than in WT mice. The results of these experiments confirm that the 5-$HT_4$ receptor is physiologically important and that function is diminished when the receptor is missing. Although a loss of the prokinetic action of the 5-$HT_4$ receptor might explain the delay in gastric emptying and slowed intestinal transit seen in KO mice, the observations are also compatible with a loss of neurons in KO mice. The most parsimonious explanation of these phenomena is that the 5-HT that is normally released from EC cells or enteric serotonergic neurons stimulates presynaptic 5-$HT_4$ receptors. These receptors enhance the amplitude of EPSCs (Galligan et al., 2003; Liu et al., 2005) and thus strengthen neurotransmission in prokinetic pathways. The difference between WT and KO mice suggests that 5-$HT_4$ receptors are required for normal GI motility. Because fewer neurons are present in the ENS of KO than WT mice, however, a paucity of neurons, as well as a presynaptic action of the 5-$HT_4$ receptor, could account for slow motility in KO mice. Although normal GI motility would thus seem to require that 5-$HT_4$ receptors be stimulated, the receptor might be needed to mediate serotonergic maintenance of the ENS instead of, or in addition to, mediating serotonergic effects on enteric neural reflexes. Long-term studies that assess the ability of 5-$HT_4$ agonists to prevent the decrease in enteric neurons by aging are in progress. The current studies suggest that it would be useful to determine whether 5-$HT_4$ agonists can be used to promote enteric neuronal survival and/or neurogenesis in human subjects with disorders that cause or result from ENS damage. Whether or not they turn out to be therapeutically valuable, the ability of 5-$HT_4$ receptors to unmask a regulation of enteric neurogenesis in adult animals suggests that the mature ENS is capable of an unexpected degree of plasticity.

## References


Abràmoff MD, Magalhães PJ, Ram SJ (2004) Image processing with ImageJ. Biophotonics Int 11:36–42.

Almond S, Lindley RM, Kenny SE, Connell MG, Edgar DH (2007) Characterization and transplantation of enteric nervous system progenitor cells. Gut 56:489–496.

Baetge G, Pintar JE, Gershon MD (1990) Transiently catecholaminergic (TC) cells in the bowel of the fetal rat: precursors of noncatecholaminergic enteric neurons. Dev Biol 141:353–380.

Barami K, Iversen K, Furneaux H, Goldman SA (1995) Hu protein as an early marker of neuronal phenotypic differentiation by subependymal zone cells of the adult songbird forebrain. J Neurobiol 28:82–101.

Beattie DT, Smith JA, Marquess D, Vickery RG, Armstrong SR, Pulido-Rios T, McCullough JL, Sandlund C, Richardson C, Mai N, Humphrey PP (2004) The 5-HT4 receptor agonist, tegaserod, is a potent 5-HT2B receptor antagonist in vitro and in vivo. Br J Pharmacol 143:549–560.

Bishop AE, Carlei F, Lee V, Trojanowski J, Marangos PJ, Dahl D, Polak JM (1985) Combined immunostaining of neurofilaments, neuron specific enolase, GFAP, and S-100. A possible method for assessing the morphological and functional status of the enteric nervous system. Histochemistry 82:93–97.

Bito H, Takemoto-Kimura S (2003) $Ca^{2+}$/CREB/CBP-dependent gene regulation: a shared mechanism critical in long-term synaptic plasticity and neuronal survival. Cell Calcium 34:425–430.

Bito H, Deisseroth K, Tsien RW (1996) CREB phosphorylation and dephosphorylation: a $Ca^{2+}$- and stimulus duration-dependent switch for hippocampal gene expression. Cell 87:1203–1214.

Bixby S, Kruger GM, Mosher JT, Joseph NM, Morrison SJ (2002) Cell-intrinsic differences between stem cells from different regions of the peripheral nervous system regulate the generation of neural diversity. Neuron 35:643–656.

Bockaert J, Claeysen S, Compan V, Dumuis A (2004) 5-HT4 receptors. Curr Drug Targets CNS Neurol Disord 3:39–51.

Bockaert J, Claeysen S, Compan V, Dumuis A (2008) 5-$HT_4$ receptors: history, molecular pharmacology and brain functions. Neuropharmacology 55:922–931.

Bondurand N, Natarajan D, Thapar N, Atkins C, Pachnis V (2003) Neuron and glia generating progenitors of the mammalian enteric nervous system isolated from fetal and postnatal gut cultures. Development 130:6387–6400.

Bredesen DE, Rao RV, Mehlen P (2006) Cell death in the nervous system. Nature 443:796–802.

Bush TG (2002) Enteric glial cells. An upstream target for induction of necrotizing enterocolitis and Crohn's disease? Bioessays 24:130–140.

Bush TG, Savidge TC, Freeman TC, Cox HJ, Campbell EA, Mucke L, Johnson MH, Sofroniew MV (1998) Fulminant jejuno-ileitis following ablation of enteric glia in adult transgenic mice. Cell 93:189–201.

Bush TG, Puvanachandra N, Horner CH, Polito A, Ostenfeld T, Svendsen CN, Mucke L, Johnson MH, Sofroniew MV (1999) Leukocyte infiltration, neuronal degeneration, and neurite outgrowth after ablation of scar-forming, reactive astrocytes in adult transgenic mice. Neuron 23:297–308.

Camilleri M, Cowen T, Koch TR (2008) Enteric neurodegeneration in ageing. Neurogastroenterol Motil 20:418–429.

Chiocchetti R, Poole DP, Kimura H, Aimi Y, Robbins HL, Castelucci P, Furness JB (2003) Evidence that two forms of choline acetyltransferase are differentially expressed in subclasses of enteric neurons. Cell Tissue Res 311:11–22.

Chou YH, Khuon S, Herrmann H, Goldman RD (2003) Nestin promotes the phosphorylation-dependent disassembly of vimentin intermediate filaments during mitosis. Mol Biol Cell 14:1468–1478.

Compan V, Zhou M, Grailhe R, Gazzara RA, Martin R, Gingrich J, Dumuis A, Brunner D, Bockaert J, Hen R (2004) Attenuated response to stress and novelty and hypersensitivity to seizures in 5-$HT_4$ receptor knock-out mice. J Neurosci 24:412–419.

Czaja K, Burns GA, Ritter RC (2008) Capsaicin-induced neuronal death and proliferation of the primary sensory neurons located in the nodose ganglia of adult rats. Neuroscience 154:621–630.

D'Autréaux F, Morikawa Y, Cserjesi P, Gershon MD (2007) Hand2 is necessary for terminal differentiation of enteric neurons from crest-derived precursors but not for their migration into the gut or for formation of glia. Development 134:2237–2249.

Deisseroth K, Bito H, Tsien RW (1996) Signaling from synapse to nucleus: postsynaptic CREB phosphorylation during multiple forms of hippocampal synaptic plasticity. Neuron 16:89–101.

del Rio JA, Soriano E (1989) Immunocytochemical detection of 5′-bromodeoxyuridine incorporation in the central nervous system of the mouse. Brain Res Dev Brain Res 49:311–317.

Dickson TC, Chung RS, McCormack GH, Staal JA, Vickers JC (2007) Acute reactive and regenerative changes in mature cortical axons following injury. Neuroreport 18:283–288.

Dumuis A, Sebben M, Bockaert J (1989a) BRL 24924: a potent agonist at a non-classical 5-HT receptor positively coupled with adenylate cyclase in colliculi neurons. Eur J Pharmacol 162:381–384.

Dumuis A, Sebben M, Bockaert J (1989b) The gastrointestinal prokinetic benzamide derivatives are agonists at the non-classical 5-HT receptor (5-$HT_4$) positively coupled to adenylate cyclase in neurons. Naunyn Schmiedebergs Arch Pharmacol 340:403–410.

Dumuis A, Sebben M, Monferini E, Nicola M, Turconi M, Ladinsky H, Bockaert J (1991) Azabicycloalkyl benzimidazolone derivatives as a novel class of potent agonists at the 5-$HT_4$ receptor positively coupled to adenylate cyclase in brain. Naunyn Schmiedebergs Arch Pharmacol 343:245–251.

Erspamer V (1966) Occurrence of indolealkylamines in nature. In: Handbook of experimental pharmacology: 5-hydroxytryptamine and related indolealkylamines (Erspamer V, ed), pp 132–181. New York: Springer.

Ertürk A, Hellal F, Enes J, Bradke F (2007) Disorganized microtubules underlie the formation of retraction bulbs and the failure of axonal regeneration. J Neurosci 27:9169–9180.

Estrada-Mondaca S, Carreón-Rodríguez A, Belkind-Gerson J (2007) Biology of the adult enteric neural stem cell. Dev Dyn 236:20–32.

Fiorica-Howells E, Maroteaux L, Gershon MD (2000) Serotonin and the 5-$HT_{2B}$ receptor in the development of enteric neurons. J Neurosci 20:294–305.

Francis F, Koulakoff A, Boucher D, Chafey P, Schaar B, Vinet MC, Friocourt G, McDonnell N, Reiner O, Kahn A, McConnell SK, Berwald-Netter Y, Denoulet P, Chelly J (1999) Doublecortin is a developmentally regulated, microtubule-associated protein expressed in migrating and differentiating neurons. Neuron 23:247–256.

Fukui T, Takeda H, Shu HJ, Ishihama K, Otake S, Suzuki Y, Nishise S, Ito N, Sato T, Togashi H, Kawata S (2006) Investigation of Musashi-1 expressing cells in the murine model of dextran sodium sulfate-induced colitis. Dig Dis Sci 51:1260–1268.

Gabella G (2001) Development and ageing of intestinal musculature and nerves: the guinea-pig taenia coli. J Neurocytol 30:733–766.

Gabella G, Trigg P (1984) Size of neurons and glial cells in the enteric ganglia of mice, guinea-pigs, rabbits and sheep. J Neurocytol 13:49–71.

Galligan JJ, Parkman H (2007) Recent advances in understanding the role of serotonin in gastrointestinal motility and functional bowel disorders. Neurogastroenterol Motil 19 [Suppl 2]:1–4.

Galligan JJ, Pan H, Messori E (2003) Signaling mechanism coupled to 5-hydroxytryptamine 4 receptor-mediated facilitation of fast synaptic transmission in the guinea-pig ileum myenteric plexus. Neurogastroenterol Motil 15:523–529.

Ganns D, Schrödl F, Neuhuber W, Brehmer A (2006) Investigation of general and cytoskeletal markers to estimate numbers and proportions of neurons in the human intestine. Histol Histopathol 21:41–51.

Gershon MD, Ratcliffe EM (2006) Development of the enteric nervous system. In: Physiology of the gastrointestinal tract, Ed 4 (Johnson LR, Barrett KE, Ghishan FK, Mechant JL, Said HM, Wood JD, eds), pp 499–521. Burlington, MA: Elsevier Academic.

Gershon MD, Tack J (2007) The serotonin signaling system: from basic understanding to drug development for functional GI disorders. Gastroenterology 132:397–414.

Geuna S, Borrione P, Filogamo G (2002) Postnatal histogenesis in the peripheral nervous system. Int J Dev Neurosci 20:475–479.

Gleeson JG, Lin PT, Flanagan LA, Walsh CA (1999) Doublecortin is a microtubule-associated protein and is expressed widely by migrating neurons. Neuron 23:257–271.

Graus F, Cordon-Cardo C, Posner JB (1985) Neuronal antinuclear antibody in sensory neuronopathy from lung cancer. Neurology 35:538–543.

Heanue TA, Pachnis V (2007) Enteric nervous system development and Hirschsprung's disease: advances in genetic and stem cell studies. Nat Rev Neurosci 8:466–479.

Herbarth B, Pingault V, Bondurand N, Kuhlbrodt K, Hermans-Borgmeyer I, Puliti A, Lemort N, Goossens M, Wegner M (1998) Mutation of the Sry-related Sox10 gene in dominant megacolon, a mouse model for human Hirschsprung's disease. Proc Natl Acad Sci U S A 95:5161–5165.

Horesh D, Sapir T, Francis F, Wolf SG, Caspi M, Elbaum M, Chelly J, Reiner O (1999) Doublecortin, a stabilizer of microtubules. Hum Mol Genet 8:1599–1610.

Inada T, Asai T, Yamada M, Shingu K (2004) Propofol and midazolam inhibit gastric emptying and gastrointestinal transit in mice. Anesth Analg 99:1102–1106.

Jean A, Conductier G, Manrique C, Bouras C, Berta P, Hen R, Charnay Y, Bockaert J, Compan V (2007) Anorexia induced by activation of serotonin 5-HT4 receptors is mediated by increases in CART in the nucleus accumbens. Proc Natl Acad Sci U S A 104:16335–16340.

Jessen KR, Mirsky R (1980) Glial cells in the enteric nervous system contain glial fibrillary acidic protein. Nature 286:736–737.

Jessen KR, Mirsky R (1985) Glial fibrillary acidic polypeptide in peripheral glia. Molecular weight, heterogeneity and distribution. J Neuroimmunol 8:377–393.

Johnson RJ, Schemann M, Santer RM, Cowen T (1998) The effects of age on the overall population and on sub-populations of myenteric neurons in the rat small intestine. J Anat 192:479–488.

Kabeya Y, Mizushima N, Ueno T, Yamamoto A, Kirisako T, Noda T, Kominami E, Ohsumi Y, Yoshimori T (2000) LC3, a mammalian homologue of yeast Apg8p, is localized in autophagosome membranes after processing. EMBO J [Erratum (2003) 22:4577] 19:5720–5728.

Kaneko Y, Sakakibara S, Imai T, Suzuki A, Nakamura Y, Sawamoto K, Ogawa Y, Toyama Y, Miyata T, Okano H (2000) Musashi1: an evolutionally conserved marker for CNS progenitor cells including neural stem cells. Dev Neurosci 22:139–153.

Key G, Kubbutat MH, Gerdes J (1994) Assessment of cell proliferation by means of an enzyme-linked immunosorbent assay based on the detection of the Ki-67 protein. J Immunol Methods 177:113–117.

Klionsky DJ, Abeliovich H, Agostinis P, Agrawal DK, Aliev G, Askew DS, Baba M, Baehrecke EH, Bahr BA, Ballabio A, Bamber BA, Bassham DC, Bergamini E, Bi X, Biard-Piechaczyk M, Blum JS, Bredesen DE, Brodsky JL, Brumell JH, Brunk UT, et al. (2008) Guidelines for the use and interpretation of assays for monitoring autophagy in higher eukaryotes. Autophagy 4:151–175.

Kraszewski K, Mundigl O, Daniell L, Verderio C, Matteoli M, De Camilli P (1995) Synaptic vesicle dynamics in living cultured hippocampal neurons visualized with CY3-conjugated antibody directed against the luminal domain of synaptotagmin. J Neurosci 15:4328–4342.

Kruger GM, Mosher JT, Bixby S, Joseph N, Iwashita T, Morrison SJ (2002) Neural crest stem cells persist in the adult gut but undergo changes in self-renewal, neuronal subtype potential, and factor responsiveness. Neuron 35:657–669.

Kurtz A, Zimmer A, Schnütgen F, Brüning G, Spener F, Müller T (1994) The expression pattern of a novel gene encoding brain-fatty acid binding protein correlates with neuronal and glial cell development. Development 120:2637–2649.

Lagares A, Li HY, Zhou XF, Avendaño C (2007) Primary sensory neuron addition in the adult rat trigeminal ganglion: evidence for neural crest glio-neuronal precursor maturation. J Neurosci 27:7939–7953.

Lambert HW, Weiss ER, Lauder JM (2001) Activation of 5-HT receptors that stimulate the adenylyl cyclase pathway positively regulates IGF-I in cultured craniofacial mesenchymal cells. Dev Neurosci 23:70–77.

Le Douarin NM, Kalcheim C (1999) The neural crest, Ed 2. Cambridge, UK: Cambridge UP.

Li HY, Say EH, Zhou XF (2007) Isolation and characterization of neural crest progenitors from adult dorsal root ganglia. Stem Cells 25:2053–2065.

Lindley RM, Hawcutt DB, Connell MG, Almond SN, Vannucchi MG, Faussone-Pellegrini MS, Edgar DH, Kenny SE (2008) Human and mouse enteric nervous system neurosphere transplants regulate the function of aganglionic embryonic distal colon. Gastroenterology 135:205–216.e6.

Liu M, Geddis MS, Wen Y, Setlik W, Gershon MD (2005) Expression and function of 5-HT4 receptors in the mouse enteric nervous system. Am J Physiol Gastrointest Liver Physiol 289:G1148–G1163.

Liu MT, Rayport S, Jiang Y, Murphy DL, Gershon MD (2002) Expression and function of 5-HT3 receptors in the enteric neurons of mice lacking the serotonin transporter. Am J Physiol Gastrointest Liver Physiol 283:G1398–G1411.

Llewellyn-Smith IJ, Costa M, Furness JB, Bornstein JC (1993) Structure of the tertiary component of the myenteric plexus in the guinea-pig small intestine. Cell Tissue Res 272:509–516.

Lucas G, Rymar VV, Du J, Mnie-Filali O, Bisgaard C, Manta S, Lambas-Senas L, Wiborg O, Haddjeri N, Piñeyro G, Sadikot AF, Debonnel G (2007) Serotonin$_4$ (5-$HT_4$) receptor agonists are putative antidepressants with a rapid onset of action. Neuron 55:712–725.

Magavi SS, Macklis JD (2008) Immunocytochemical analysis of neuronal differentiation. Methods Mol Biol 438:345–352.

Maka M, Stolt CC, Wegner M (2005) Identification of Sox8 as a modifier gene in a mouse model of Hirschsprung disease reveals underlying molecular defect. Dev Biol 277:155–169.

Marusich MF, Weston JA (1992) Identification of early neurogenic cells in the neural crest lineage. Dev Biol 149:295–306.

May R, Riehl TE, Hunt C, Sureban SM, Anant S, Houchen CW (2008) Identification of a novel putative gastrointestinal stem cell and adenoma stem cell marker, doublecortin and CaM kinase-like-1, following radiation injury and in adenomatous polyposis coli/multiple intestinal neoplasia mice. Stem Cells 26:630–637.

Miller MS, Galligan JJ, Burks TF (1981) Accurate measurement of intestinal transit in the rat. J Pharmacol Methods 6:211–217.

Miller MW, Nowakowski RS (1988) Use of bromodeoxyuridine-immunohistochemistry to examine the proliferation, migration and time of origin of cells in the central nervous system. Brain Res 457:44–52.

Montminy M (1997) Transcriptional regulation by cyclic AMP. Annu Rev Biochem 66:807–822.
Moore BA, Otterbein LE, Türler A, Choi AM, Bauer AJ (2003) Inhaled carbon monoxide suppresses the development of postoperative ileus in the murine small intestine. Gastroenterology 124:377–391.
Mullen RJ, Buck CR, Smith AM (1992) NeuN, a neuronal specific nuclear protein in vertebrates. Development 116:201–211.
Nagata T, Kanno R, Kurihara Y, Uesugi S, Imai T, Sakakibara S, Okano H, Katahira M (1999) Structure, backbone dynamics and interactions with RNA of the C-terminal RNA-binding domain of a mouse neural RNA-binding protein, Musashi1. J Mol Biol 287:315–330.
Nakagawa S, Kim JE, Lee R, Chen J, Fujioka T, Malberg J, Tsuji S, Duman RS (2002) Localization of phosphorylated cAMP response element-binding protein in immature neurons of adult hippocampus. J Neurosci 22:9868–9876.
Nishimura S, Wakabayashi N, Toyoda K, Kashima K, Mitsufuji S (2003) Expression of Musashi-1 in human normal colon crypt cells: a possible stem cell marker of human colon epithelium. Dig Dis Sci 48:1523–1529.
Nowakowski RS, Lewin SB, Miller MW (1989) Bromodeoxyuridine immunohistochemical determination of the lengths of the cell cycle and the DNA-synthetic phase for an anatomically defined population. J Neurocytol 18:311–318.
Okano HJ, Darnell RB (1997) A hierarchy of Hu RNA binding proteins in developing and adult neurons. J Neurosci 17:3024–3037.
Pattyn A, Morin X, Cremer H, Goridis C, Brunet J-F (1999) The homeobox gene *Phox2b* is essential for the development of autonomic neural crest derivatives. Nature 399:366–370.
Pham TD, Gershon MD, Rothman TP (1991) Time of origin of neurons in the murine enteric nervous system: sequence in relation to phenotype. J Comp Neurol 314:789–798.
Phillips RJ, Powley TL (2007) Innervation of the gastrointestinal tract: patterns of aging. Auton Neurosci 136:1–19.
Phillips RJ, Hargrave SL, Rhodes BS, Zopf DA, Powley TL (2004) Quantification of neurons in the myenteric plexus: an evaluation of putative pan-neuronal markers. J Neurosci Methods 133:99–107.
Pomeranz HD, Rothman TP, Chalazonitis A, Tennyson VM, Gershon MD (1993) Neural crest-derived cells isolated from the gut by immunoselection develop neuronal and glial phenotypes when cultured on laminin. Dev Biol 156:341–361.
Poole DP, Xu B, Koh SL, Hunne B, Coupar IM, Irving HR, Shinjo K, Furness JB (2006) Identification of neurons that express 5-hydroxytryptamine4 receptors in intestine. Cell Tissue Res 325:413–422.
Portier MM, de Néchaud B, Gros F (1983) Peripherin, a new member of the intermediate filament protein family. Dev Neurosci 6:335–344.
Potten CS, Booth C, Tudor GL, Booth D, Brady G, Hurley P, Ashton G, Clarke R, Sakakibara S, Okano H (2003) Identification of a putative intestinal stem cell and early lineage marker; musashi-1. Differentiation 71:28–41.
Rao MS, Shetty AK (2004) Efficacy of doublecortin as a marker to analyze the absolute number and dendritic growth of newly generated neurons in the adult dentate gyrus. Eur J Neurosci 19:234–246.
Santer RM, Baker DM (1988) Enteric neuron numbers and sizes in Auerbach's plexus in the small and large intestine of adult and aged rats. J Auton Nerv Syst 25:59–67.
Schnütgen F, Börchers T, Müller T, Spener F (1996) Heterologous expression and characterisation of mouse brain fatty acid binding protein. Biol Chem Hoppe Seyler 377:211–215.
Southard-Smith EM, Kos L, Pavan WJ (1998) Sox10 mutation disrupts neural crest development in Dom Hirschsprung mouse model. Nat Genet 18:60–64.
Steinert PM, Chou YH, Prahlad V, Parry DA, Marekov LN, Wu KC, Jang SI, Goldman RD (1999) A high molecular weight intermediate filament-associated protein in BHK-21 cells is nestin, a type VI intermediate filament protein. Limited co-assembly in vitro to form heteropolymers with type III vimentin and type IV alpha-internexin. J Biol Chem 274:9881–9890.
Stolt CC, Lommes P, Sock E, Chaboissier MC, Schedl A, Wegner M (2003) The Sox9 transcription factor determines glial fate choice in the developing spinal cord. Genes Dev 17:1677–1689.
Takahashi T, Qoubaitary A, Owyang C, Wiley JW (2000) Decreased expression of nitric oxide synthase in the colonic myenteric plexus of aged rats. Brain Res 883:15–21.
Taupin P (2007) BrdU immunohistochemistry for studying adult neurogenesis: paradigms, pitfalls, limitations, and validation. Brain Res Rev 53:198–214.
Torres GE, Chaput Y, Andrade R (1995) Cyclic AMP and protein kinase A mediate 5-hydroxytryptamine type 4 receptor regulation of calcium-activated potassium current in adult hippocampal neurons. Mol Pharmacol 47:191–197.
Troy CM, Brown K, Greene LA, Shelanski ML (1990) Ontogeny of the neuronal intermediate filament protein, peripherin, in the mouse embryo. Neuroscience 36:217–237.
Van Nassauw L, Wu M, De Jonge F, Adriaensen D, Timmermans JP (2005) Cytoplasmic, but not nuclear, expression of the neuronal nuclei (NeuN) antibody is an exclusive feature of Dogiel type II neurons in the guinea-pig gastrointestinal tract. Histochem Cell Biol 124:369–377.
Vannucchi MG, Corsani L, Bani D, Faussone-Pellegrini MS (2002) Myenteric neurons and interstitial cells of Cajal of mouse colon express several nitric oxide synthase isoforms. Neurosci Lett 326:191–195.
Viola H, Furman M, Izquierdo LA, Alonso M, Barros DM, de Souza MM, Izquierdo I, Medina JH (2000) Phosphorylated cAMP response element-binding protein as a molecular marker of memory processing in rat hippocampus: effect of novelty. J Neurosci 20:RC112(1–5).
Wade PR, Cowen T (2004) Neurodegeneration: a key factor in the ageing gut. Neurogastroenterol Motil 16 [Suppl 1]:19–23.
Wang JW, David DJ, Monckton JE, Battaglia F, Hen R (2008) Chronic fluoxetine stimulates maturation and synaptic plasticity of adult-born hippocampal granule cells. J Neurosci 28:1374–1384.
Ward SM, Xue C, Shuttleworth CW, Bredt DS, Snyder SH, Sanders KM (1992) NADPH diaphorase and nitric oxide synthase colocalization in enteric neurons of canine proximal colon. Am J Physiol 263:G277–G284.
Wilkinson KD, Lee KM, Deshpande S, Duerksen-Hughes P, Boss JM, Pohl J (1989) The neuron-specific protein PGP 9.5 is a ubiquitin carboxyl-terminal hydrolase. Science 246:670–673.
Wojtowicz JM, Kee N (2006) BrdU assay for neurogenesis in rodents. Nat Protoc 1:1399–1405.
Yoshihara M, Adolfsen B, Galle KT, Littleton JT (2005) Retrograde signaling by Syt 4 induces presynaptic release and synapse-specific growth. Science 310:858–863.
Young HM, Bergner AJ, Müller T (2003) Acquisition of neuronal and glial markers by neural crest-derived cells in the mouse intestine. J Comp Neurol 456:1–11.
Young HM, Turner KN, Bergner AJ (2005) The location and phenotype of proliferating neural-crest-derived cells in the developing mouse gut. Cell Tissue Res 320:1–9.
Young JK, Baker JH, Muller T (1996) Immunoreactivity for brain-fatty acid binding protein in gomori-positive astrocytes. Glia 16:218–226.
Zhao C, Deng W, Gage FH (2008) Mechanisms and functional implications of adult neurogenesis. Cell 132:645–660.